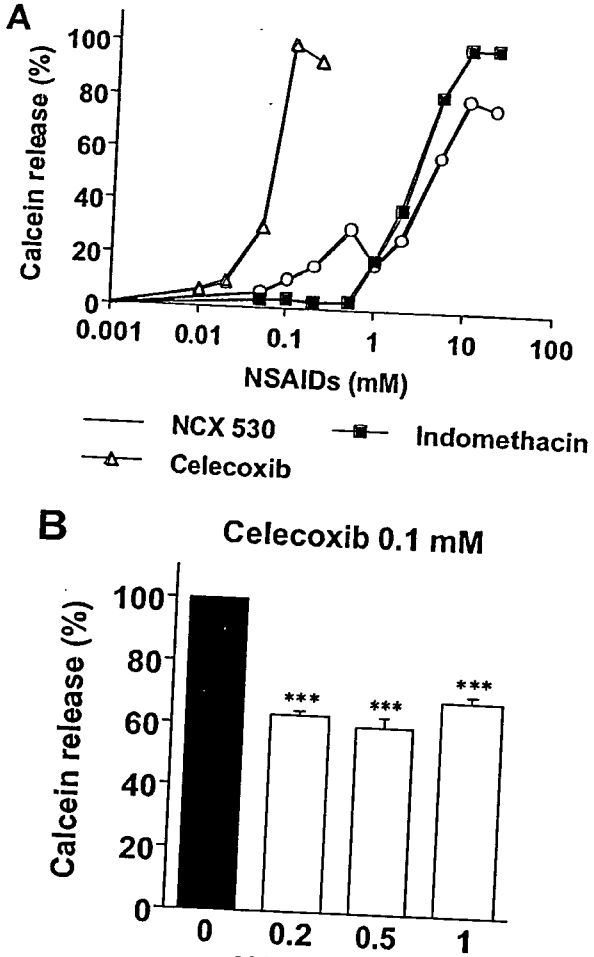

Fig 4. Membrane permeabilization by NSAIDs. Calcein-loaded liposomes were incubated for 10 min at 30°C with indicated concentrations of each NSAID (A) or 0.1 mM celecoxib plus indicated concentrations of NCX 530 (B). The release of calcein from liposomes was determined by measuring fluorescence intensity. Melittin (10 μM) was used to determine the 100% level of membrane permeabilization (47).

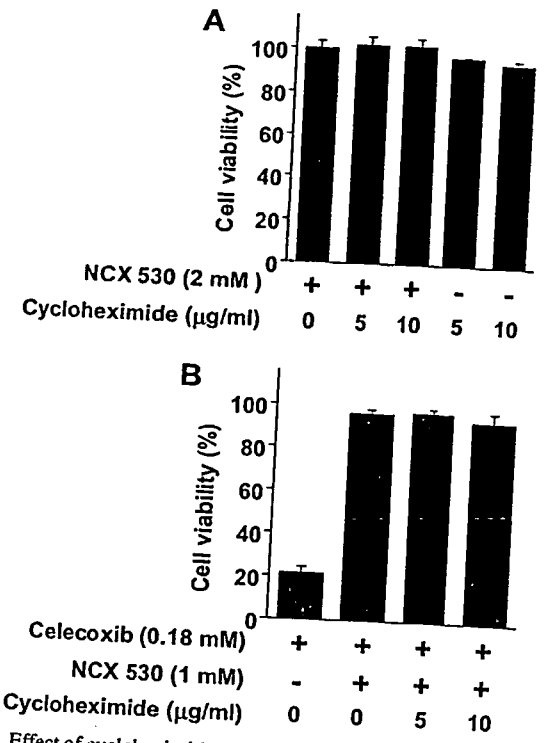

Fig 5. Effect of cycloheximide on cell viability in the presence of NCX 530. Cultured guinea pig gastric mucosal cells were pre-incubated with indicated concentrations of cycloheximide for 1 hr. Cells were further incubated with 2 mM NCX 530 and indicated concentrations of cycloheximide for 1 hr (A) (necrotic conditions). Cells were pre-incubated with indicated concentrations of cycloheximide and 1 mM NCX 530 for 1 hr. Cells were further incubated with 1 mM NCX 530, 0.18 mM celecoxib and indicated concentrations of cycloheximide for 1 hr (B) (necrotic conditions). Cell viability was determined by the MTT method. Values are mean ± S.E.M. ($n = 3$).

NCX 530 on celecoxib-induced cell death probably involves changes to the membrane permeabilizing capacity of celecoxib. However, at present, it is unclear why NCX 530 with membrane permeabilizing activity itself, protects membrane from celecoxib but not from indomethacin.

NSAIDs have been shown to stimulate the induction of some protective proteins such as heat shock proteins (33) and endoplasmic reticulum chaperons (34). It is possible that induction of protective proteins mediates the low cytotoxicity and the cytoprotective effect of NCX 530. In order to test this possibility, we examined the effect of an inhibitor of protein synthesis (cycloheximide) on the low cytotoxicity and cytoprotective effects of NCX 530. Pre-treatment of cells with cycloheximide did not affect cell viability after incubation with NCX 530 for 1 hr (necrotic conditions) (Figure 5A). Furthermore, pre-treatment of cells with cycloheximide did not affect the protective action of NCX 530 against celecoxib-induced cell death (necrotic conditions) (Figure 5B). This concentration of cycloheximide did not affect the cell viability by itself but inhibited protein synthesis, the incorporation of [^{35}S]methionine into acid-insoluble fractions to more than 90%. Since cycloheximide itself inhibits apoptosis, we could not examine its effect on NCX 530-induced apoptosis or the cytoprotective effect of NCX 530 on apoptosis. The results, however, suggest that proteins newly synthesized in the presence of NCX 530 do not contribute to the low level of NCX 530-induced necrosis or to the cytoprotective effect of NCX 530 on celecoxib-induced necrosis.

NO stimulates guanylate cyclase, resulting in an increase in cGMP. Since an increase in cGMP in cells is known to inhibit apoptosis via the inhibition of caspase-3 (35), it is possible that activation of guanylate cyclase

by NCX 530 is responsible for its low cytotoxicity and cytoprotective effects. In order to test this possibility, the effect of an inhibitor of guanylate cyclase (ODQ) on cell death in the presence of NCX 530 was examined. Pre-treatment of cells with ODQ did not affect the cell viability after treatment with NCX 530 for 1 hr (necrotic conditions) (Figure 6A). Furthermore, pre-treatment of cells with ODQ did not alter the extent of cell death induced by celecoxib in the presence NCX 530 for 1 hr (necrotic conditions) (Figure 6B). On the other hand, when the incubation period was changed to 16 hr (apoptotic conditions), pre-treatment of cells with ODQ decreased the cell viability following treatment with NCX 530 (apoptotic conditions) (Figure 6C) and increased the level of cell death induced by celecoxib in the presence NCX 530 (apoptotic conditions) (Figure 6D). This concentration of ODQ did not affect the cell viability by itself (data not shown), however, it is enough to almost completely inhibit guanylate cyclase, based on previous papers (36, 37). These results suggest that activation of guanylate cyclase by NCX 530 may play an important role in the low cytotoxic activity and the cytoprotective effect of NCX 530 for apoptosis, but not for necrosis.

Production of Gastric Lesions by NCX 530. The low cytotoxicity of NCX 530 suggests that it is less likely to produce gastric lesions *in vivo*. As shown in Figure 7, orally administered NCX 530 (42.7 mg/kg) did not produce gastric lesions to any significant extent, whereas orally administered indomethacin (30 mg/kg) (equal molar) clearly produced gastric lesions. This finding is consistent with a previous report (17) and shows that, in relation to its effects on the gastric mucosa in vivo, NCX 530 is safe for use.

As described in the introduction section, we recently found that gastric lesions develop in a manner that depends on both intravenously administered low doses of indomethacin and orally administered cytotoxic COX-2 selective inhibitors, such as celecoxib (16). Using this model, the ability of NCX 530 and indomethacin to produce gastric lesions was tested when either of these compounds was used in combination with the oral administration of celecoxib. Here, NCX 530 and indomethacin were administered intraperitoneally. As shown in Figure 8, the oral administration of celecoxib alone or the intraperitoneal administration of a low dose (5 mg/kg) of indomethacin alone did not produce gastric lesions to any significant extent; however, simultaneous administration of both compounds clearly produced gastric lesions as previously reported (16). In contrast, gastric lesions were not produced when the oral administration of celecoxib and the intraperitoneal administration of NCX 530 were used in combination (Figure 8). Furthermore, intraperitoneally

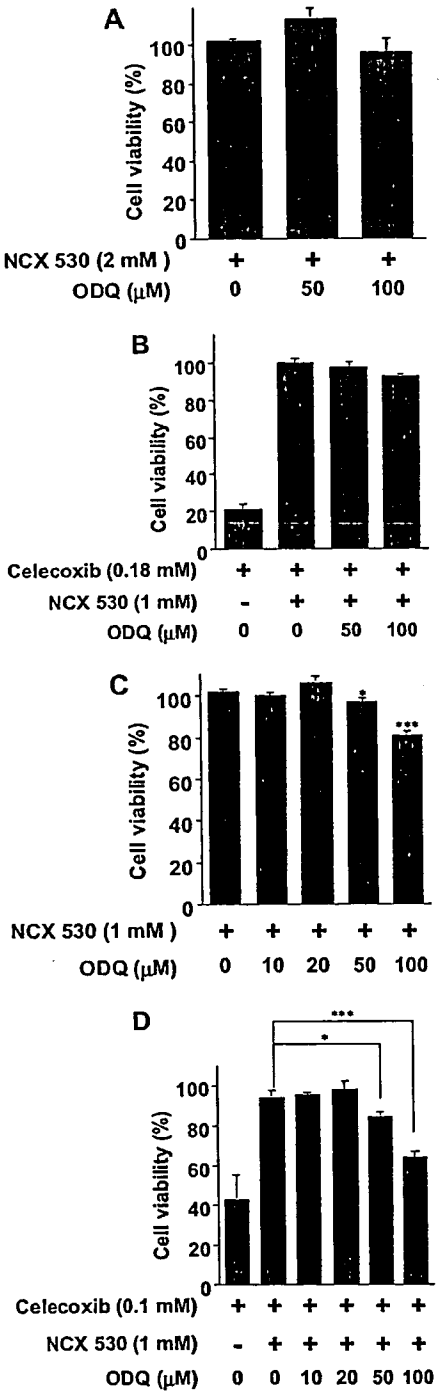

Fig 6. Effect of ODQ on cell viability in the presence of NCX 530. Cultured guinea pig gastric mucosal cells were pre-incubated with indicated concentrations of ODQ for 1 hr. Cells were further incubated with indicated concentrations of NCX 530 and ODQ (A, C). Cells were pre-incubated with indicated concentrations of ODQ and 1 mM NCX 530 for 1 hr. Cells were further incubated indicated concentrations of ODQ, NCX 530 and celecoxib (B, D). Incubation was performed for 1 hr (A, B) (necrotic conditions) or for 16 hr (C, D) (apoptotic conditions). Cell viability was determined by the MTT method. Values are mean ± S.E.M. ($n = 3$). ***$P < 0.001$; *$P < 0.05$.

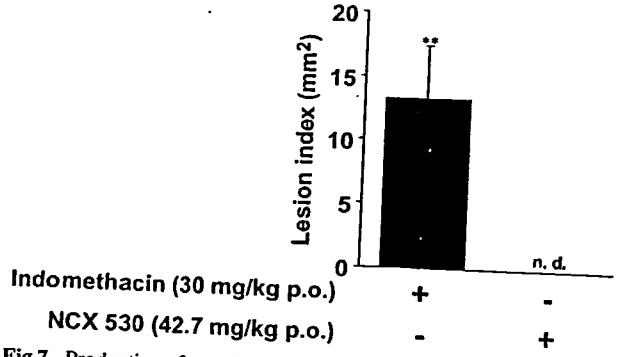

Fig 7. Production of gastric lesions by NCX 530 or indomethacin. Rats were orally administered with NCX 530 or indomethacin as indicated. After 6 hr, the stomach was removed and scored for hemorrhagic damage. Values are mean ± S.E.M. ($n = 5$–6). $^{**}P < 0.01$. n.d.; not detected.

administered NCX 530 suppressed the production of gastric lesions following the oral administration of celecoxib together with the intraperitoneal administration of indomethacin (Figure 8).

We also examined the effect of the intraperitoneal administration of NCX 530 on the production of gastric lesions by other gastric irritants. As shown in Figure 9A, NCX 530 administered in this way significantly decreased the ethanol-induced production of gastric lesions. In contrast, gastric lesions were clearly apparent when indomethacin was administered in place of NCX 530 (Figure 9A). On the other hand, the intraperitoneal administration of NCX 530 did not affect the production of gastric lesions following the oral administration of high doses (30 mg/kg)

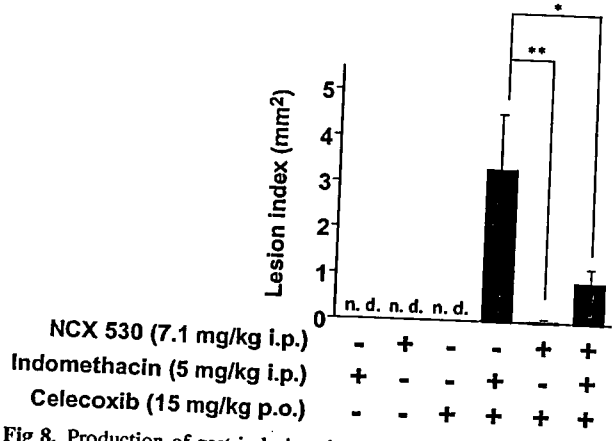

Fig 8. Production of gastric lesions by NCX 530 or indomethacin in combination with celecoxib. Rats were intraperitoneally administered with 5 mg/kg indomethacin or 7.1 mg/kg NCX 530 or vehicle. After 1 hr, animals were administered orally with 15 mg/mL celecoxib or vehicle. After 6 hr, the stomach was removed and scored for hemorrhagic damage. Values are mean ± S.E.M. ($n = 5 - 6$). $^{**}P < 0.01$; $^{*}P < 0.05$. n.d.; not detected.

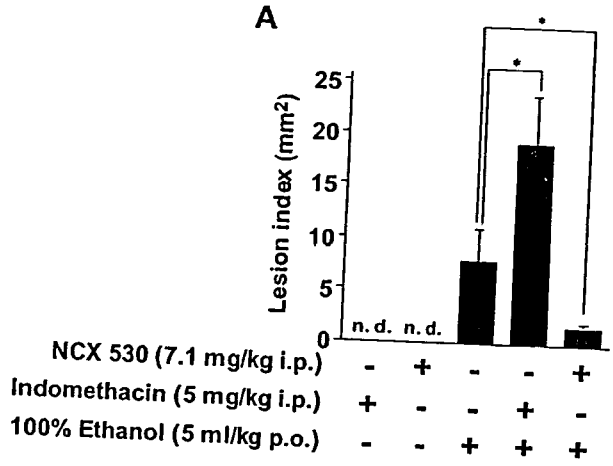

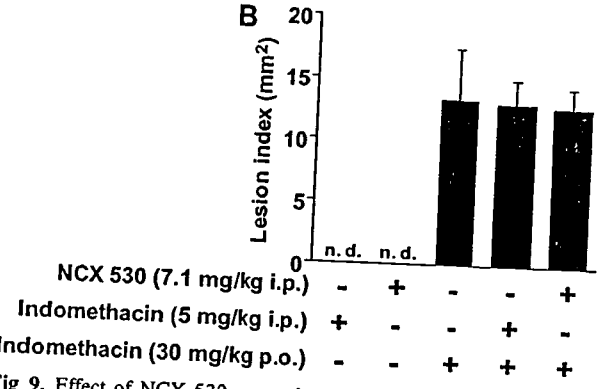

Fig 9. Effect of NCX 530 on production of gastric lesions by other gastric irritants. Rats were intraperitoneally administered with 7.1 mg/kg NCX 530 or 5 mg/kg indomethacin or vehicle. After 1 hr, animals were administered orally with ethanol (A) or 30 mg/kg indomethacin (B) or vehicle. After 6 hr, the stomach was removed and scored for hemorrhagic damage. Values are mean ± S.E.M. ($n = 5$–6). $^{*}P < 0.05$. n.d.; not detected.

of indomethacin (Figure 9B). Therefore, NCX 530 can suppress the production of gastric lesions by some but not all gastric irritants.

DISCUSSION

In this study, the cytotoxicity of NCX 530, one of the new breed of NO-NSAIDs, was assessed. NCX 530 induced both necrosis and apoptosis in gastric mucosal cells in primary culture at much lower levels than did indomethacin. These results are apparently inconsistent with recently published results (38). This may be due to the difference in species of cells and NO-indomethacin; they used colon cancer cells and another NO-indomethacin (NCX 2121) (38). The cytotoxicity of an irritant is determined by both its own toxicity and its capacity to induce cellular stress responses, which, in turn, protect cells from

the irritant. The low cytotoxicity of NCX 530, however, could not be explained by its own toxicity given that NCX 530 gave rise to a similar degree of membrane permeabilization as that seen for indomethacin. On the other hand, a cGMP-dependent cellular response could be involved in the low level induction of apoptosis by NCX 530, since an inhibitor of guanylate cyclase (ODQ) stimulated apoptosis in the presence of NCX 530.

We also found that NCX 530 protects gastric mucosal cells from celecoxib-induced necrosis and apoptosis. This cytoprotective effect of NCX 530 involved both membrane permeabilization and a cGMP-dependent cellular stress response; NCX 530 partially suppressed celecoxib-dependent membrane permeabilization and ODQ inhibited the NCX 530-dependent protection of cells from celecoxib-induced necrosis and apoptosis. However, the reason why NCX 530 protects cells from some irritants (celecoxib, ethanol), but not others (indomethacin, hydrogen peroxide) is yet to be determined. Since the suppression by ODQ of the cytoprotective effect of NCX 530 was partial, other mechanisms may be involved in this cytoprotection. In addition to membrane permeabilization, stimulation of mucus synthesis by NCX 530 may be involved in this cytoprotection as suggested previously (39).

We recently proposed that not only COX inhibition but also the direct cytotoxic effect of NSAIDs (direct cell damage at the gastric mucosa) is involved in the development of gastric lesions (16). On this basis, we proposed that NSAIDs that did not inhibit COX at the gastric mucosa or were without direct cytotoxic effects would not be capable of producing gastric lesions (16). Selective COX-2 inhibitors are NSAIDs that do not inhibit COX at the gastric mucosa, keeping in mind that the primary form of COX expressed at the gastric mucosa is COX-1. However, a recently raised issue concerning the use of selective COX-2 inhibitors is their potential risk for cardiovascular thrombotic events, which is caused by their specificity for COX-2 (40–46). As such, we proposed that NSAIDs without both specificity for COX-2 and direct cytotoxicity are safe for use from a viewpoint of the gastric mucosa and cardiovascular system and therefore have important advantages for clinical use (16). Based on results of this study, NCX 530 may belong to this category of NSAIDs.

A combination of the oral administration of celecoxib with the intraperitoneal administration of NCX 530 did not produce gastric lesions, which is different from the case of intraperitoneal administration of indomethacin. Furthermore, NCX 530 administered intraperitoneally suppressed the production of gastric lesions induced by ethanol or celecoxib plus indomethacin. Since many factors can affect the production of gastric lesions in vivo (mucosal blood flow and gastric motility for example), a number of interpretations for this phenomenon are possible. However, we consider that the direct cytotoxicity of NSAIDs, or direct cell damage at the gastric mucosa by NSAIDs in other words, can explain this phenomenon. In gastric lesions produced by a combination of the oral administration of celecoxib with the intraperitoneal administration of indomethacin or NCX 530, the direct cell damage at gastric mucosa should occur on account of the orally administered celecoxib. As shown in vitro, NCX 530 may suppress celecoxib-induced cell death at the gastric mucosa, meaning that NCX 530 does not actually produce gastric lesions when administered in conjunction with the celecoxib. This idea can also be used to explain the NCX 530-dependent suppression of the production of gastric lesions by ethanol or celecoxib plus indomethacin, given that, in vitro, NCX 530 protected the gastric mucosal cells not only from celecoxib but also from ethanol. Furthermore, observations that NCX 530 did not protect gastric mucosal cells from indomethacin in vitro may explain why the production of gastric lesions by the oral administration of high doses of indomethacin was not suppressed by NCX 530 in vivo. However, in Figure 8, NCX 530 almost completely inhibited the production of gastric lesions by celecoxib in vivo, whereas the effect of this drug on celecoxib-induced cell death is partial in vitro (Figures 2A and 3A). Previous papers reported that NCX 530 stimulated mucosal blood flow and mucus synthesis and did not so clearly increase gastric motility and adhesion of neutrophil as indomethacin (17, 39). We consider that these phenomenon are involved in the safety of NCX 530 on gastric mucosa in vivo.

ACKNOWLEDGMENTS

This work was supported by Grants-in-Aid for Scientific Research from the Ministry of Health, Labour, and Welfare of Japan, as well as by the Suzuken Memorial Foundation, and the Japan Research Foundation for Clinical Pharmacology. We thank NicOx S. A. for providing indomethacin and NCX 530.

REFERENCES

1. Smalley WE, Ray WA, Daugherty JR, Griffin MR: Nonsteroidal anti-inflammatory drugs and the incidence of hospitalizations for peptic ulcer disease in elderly persons. Am J Epidemiol 141:539–545, 1995
2. Hawkey CJ: Nonsteroidal anti-inflammatory drug gastropathy. Gastroenterology 119:521–535, 2000
3. Barrier CH, Hirschowitz BI: Controversies in the detection and management of nonsteroidal antiinflammatory drug-induced side effects of the upper gastrointestinal tract. Arthritis Rheum 32:926–932, 1989
4. Gabriel SE, Jaakkimainen L, Bombardier C: Risk for serious gastrointestinal complications related to use of nonsteroidal

anti-inflammatory drugs. A meta-analysis. Ann Intern Med 115:787–796, 1991
5. Fries JF, Miller SR, Spitz PW, Williams CA, Hubert HB, Bloch DA: Toward an epidemiology of gastropathy associated with nonsteroidal antiinflammatory drug use. Gastroenterology 96:647–655, 1989
6. Kurata JH, Abbey DE: The effect of chronic aspirin use on duodenal and gastric ulcer hospitalizations. J Clin Gastroenterol 12:260–266, 1990
7. Singh G: Recent considerations in nonsteroidal anti-inflammatory drug gastropathy. Am J Med 105:31S–38S, 1998
8. Vane JR, Botting RM: Mechanism of action of anti-inflammatory drugs. Scand J Rheumatol (Suppl 102):9–21, 1996
9. Miller TA: Protective effects of prostaglandins against gastric mucosal damage: current knowledge and proposed mechanisms. Am J Physiol 245:G601–G623, 1983
10. Ligumsky M, Golanska EM, Hansen DG, Kauffman GJ: Aspirin can inhibit gastric mucosal cyclo-oxygenase without causing lesions in rat. Gastroenterology 84:756–761, 1983
11. Ligumsky M, Sestieri M, Karmeli F, Zimmerman J, Okon E, Rachmilewitz D: Rectal administration of nonsteroidal antiinflammatory drugs. Effect on rat gastric ulcerogenicity and prostaglandin E2 synthesis. Gastroenterology 1245–1249, 1990
12. Lichtenberger LM: Where is the evidence that cyclooxygenase inhibition is the primary cause of nonsteroidal anti-inflammatory drug (NSAID)-induced gastrointestinal injury? Topical injury revisited. Biochem Pharmacol 61:631–637, 2001
13. Lichtenberger LM, Wang ZM, Romero JJ, Ulloa C, Perez JC, Giraud MN, Barreto JC: Non-steroidal anti-inflammatory drugs (NSAIDs) associate with zwitterionic phospholipids: insight into the mechanism and reversal of NSAID-induced gastrointestinal injury. Nat Med 1:154–158, 1995
14. Somasundaram S, Rafi S, Hayllar J, Sigthorsson G, Jacob M, Price AB, Macpherson A, Mahmod T, Scott D, Wrigglesworth JM, Bjarnason I: Mitochondrial damage: a possible mechanism of the "topical" phase of NSAID induced injury to the rat intestine. Gut 41:344–353, 1997
15. Tomisato W, Tsutsumi S, Rokutan K, Tsuchiya T, Mizushima T: NSAIDs induce both necrosis and apoptosis in guinea pig gastric mucosal cells in primary culture. Am J Physiol Gastrointest Liver Physiol 281:G1092–G1100, 2001
16. Tomisato W, Tsutsumi S, Hoshino T, Hwang HJ, Mio M, Tsuchiya T, Mizushima T: Role of direct cytotoxic effects of NSAIDs in the induction of gastric lesions. Biochem Pharmacol 67:575–585, 2004
17. Takeuchi K, Mizoguchi H, Araki H, Komoike Y, Suzuki K: Lack of gastric toxicity of nitric oxide-releasing indomethacin, NCX-530, in experimental animals. Dig Dis Sci 46:1805–1818, 2001
18. Hawkey CJ, Jones JI, Atherton CT, Skelly MM, Bebb JR, Fagerholm U, Jonzon B, Karlsson P, Bjarnason IT: Gastrointestinal safety of AZD3582, a cyclooxygenase inhibiting nitric oxide donator: proof of concept study in humans. Gut 52:1537–1542, 2003
19. Johnson AJ, Hsu AL, Lin HP, Song X, Chen CS: The cyclooxygenase-2 inhibitor celecoxib perturbs intracellular calcium by inhibiting endoplasmic reticulum Ca^{2+}-ATPases: a plausible link with its anti-tumour effect and cardiovascular risks. Biochem J 366:831–837, 2002
20. Fiorucci S, Santucci L, Gresele P, Faccino RM, Del Soldato P, Morelli A: Gastrointestinal safety of NO-aspirin (NCX-4016) in healthy human volunteers: a proof of concept endoscopic study. Gastroenterology 124:600–607, 2003
21. Wallace JL, Reuter B, Cicala C, McKnight W, Grisham MB, Cirino G: Novel nonsteroidal anti-inflammatory drug derivatives with markedly reduced ulcerogenic properties in the rat. Gastroenterology 107:173–179, 1994
22. Wallace JL, McKnight W, Del Soldato P, Baydoun AR, Cirino G: Anti-thrombotic effects of a nitric oxide-releasing, gastric-sparing aspirin derivative. J Clin Invest 96:2711–2718, 1995
23. Wallace JL, Miller MJ: Nitric oxide in mucosal defense: a little goes a long way. Gastroenterology 119:512–520, 2000
24. Johal K, Hanson PJ: Opposite effects of flurbiprofen and the nitroxybutyl ester of flurbiprofen on apoptosis in cultured guinea-pig gastric mucous cells. Br J Pharmacol 130:811–818, 2000
25. Fiorucci S, Santucci L, Federici B, Antonelli E, Distrutti E, Morelli O, Renzo GD, Coata G, Cirino G, Soldato PD, Morelli A: Nitric oxide-releasing NSAIDs inhibit interleukin-1beta converting enzyme-like cysteine proteases and protect endothelial cells from apoptosis induced by TNFalpha. Aliment Pharmacol Ther 13:421–435, 1999
26. Hirakawa T, Rokutan K, Nikawa T, Kishi K: Geranylgeranylacetone induces heat shock proteins in cultured guinea pig gastric mucosal cells and rat gastric mucosa. Gastroenterology 111:345–357, 1996
27. Tomisato W, Takahashi N, Komoto C, Rokutan K, Tsuchiya T, Mizushima T: Geranylgeranylacetone protects cultured guinea pig gastric mucosal cells from indomethacin. Dig Dis Sci 45:1674–1679, 2000
28. Tomisato W, Hoshino T, Tsutsumi S, Tsuchiya T, Mizushima T: Maturation-associated increase in sensitivity of cultured guinea pig gastric pit cells to hydrogen peroxide. Dig Dis Sci 47:2125–2133, 2002
29. Tsutsumi S, Tomisato W, Takano T, Rokutan K, Tsuchiya T, Mizushima T: Gastric irritant-induced apoptosis in guinea pig gastric mucosal cells in primary culture. Biochim Biophys Acta 1589:168–180, 2002
30. Katsu T: Application of calcein-loaded liposomes for the determination of membrane channel size. Biol Pharm Bull 22:978–980, 1999
31. New RRC: Liposomes: A Practical Approach. Oxford: IRL Press, 1990, pp 105–161.
32. Tomisato W, Tanaka K, Katsu T, Kakuta H, Sasaki K, Tsutsumi S, Hoshino T, Aburaya M, Li D, Tsuchiya T, Suzuki K, Yokomizo K, Mizushima T: Membrane permeabilization by non-steroidal anti-inflammatory drugs. Biochem Biophys Res Commun 323:1032–1039, 2004
33. Lee BS, Chen J, Angelidis C, Jurivich DA, Morimoto RI: Pharmacological modulation of heat shock factor 1 by antiinflammatory drugs results in protection against stress-induced cellular damage. Proc Natl Acad Sci USA 92:7207–7211, 1995
34. Tsutsumi S, Gotoh T, Tomisato W, Mima S, Hoshino T, Hwang HJ, Takenaka H, Tsuchiya T, Mori M, Mizushima T: Endoplasmic reticulum stress response is involved in nonsteroidal anti-inflammatory drug-induced apoptosis. Cell Death Differ, 2004
35. Kim YM, Talanian RV, Billiar TR: Nitric oxide inhibits apoptosis by preventing increases in caspase-3-like activity via two distinct mechanisms. J Biol Chem 272:31138–31148, 1997
36. Brunner F, Stessel H, Kukovetz WR: Novel guanylyl cyclase inhibitor, ODQ reveals role of nitric oxide, but not of cyclic GMP in endothelin-1 secretion. FEBS Lett 376:262–266, 1995
37. Fiorucci S, Antonelli E, Santucci L, Morelli O, Miglietti M, Federici B, Mannucci R, Del Soldato P, Morelli A: Gastrointestinal safety of nitric oxide-derived aspirin is related to inhibition of ICE-like cysteine proteases in rats. Gastroenterology 116:1089–1106, 1999
38. Yeh RK, Chen J, Williams JL, Baluch M, Hundley TR, Rosenbaum RE, Kalala S, Traganos F, Benardini F, del Soldato P, Kashfi K, Rigas

B: NO-donating nonsteroidal antiinflammatory drugs (NSAIDs) inhibit colon cancer cell growth more potently than traditional NSAIDs: a general pharmacological property? Biochem Pharmacol 67:2197–2205, 2004
39. Mizoguchi H, Hase S, Tanaka A, Takeuchi K: Lack of small intestinal ulcerogenecity of nitric oxide-releasing indomethacin, NCX-530, in rats. Aliment Pharmacol Ther 15:257–267, 2001
40. Mukherjee D, Nissen SE, Topol EJ: Risk of cardiovascular events associated with selective COX-2 inhibitors. JAMA 286:954–959, 2001
41. Mukherjee D: Selective cyclooxygenase-2 (COX-2) inhibitors and potential risk of cardiovascular events. Biochem Pharmacol 63:817–821, 2002
42. McAdam BF, Catella LF, Mardini IA, Kapoor S, Lawson JA, Fitzgerald GA: Systemic biosynthesis of prostacyclin by cyclooxygenase (COX)-2: the human pharmacology of a selective inhibitor of COX-2. Proc Natl Acad Sci USA 96:272–277, 1999
43. Catella LF, McAdam B, Morrison BW, Kapoor S, Kujubu D, Antes L, Lasseter KC, Quan H, Gertz BJ, Fitzgerald GA: Effects of specific inhibition of cyclooxygenase-2 on sodium balance, hemodynamics, and vasoactive eicosanoids. J Pharmacol Exp Ther 289:735–741, 1999
44. Belton O, Byrne D, Kearney D, Leahy A, Fitzgerald DJ: Cyclooxygenase-1 and -2-dependent prostacyclin formation in patients with atherosclerosis. Circulation 102:840–845, 2000
45. Hennan JK, Huang J, Barrett TD, Driscoll EM, Willens DE, Park AM, Crofford LJ, Lucchesi BR: Effects of selective cyclooxygenase-2 inhibition on vascular responses and thrombosis in canine coronary arteries. Circulation 104:820–825, 2001
46. Dowd NP, Scully M, Adderley SR, Cunningham AJ, Fitzgerald DJ: Inhibition of cyclooxygenase-2 aggravates doxorubicin-mediated cardiac injury in vivo. J Clin Invest 108:585–590, 2001
47. Katsu T, Kobayashi H, Hirota T, Fujita Y, Sato K, Nagai U: Structure–activity relationship of gramicidin S analogues on membrane permeability. Biochim Biophys Acta 899:159–170, 1987

Available online at www.sciencedirect.com
SCIENCE DIRECT®
Hearing Research 204 (2005) 140–146
HEARING RESEARCH
www.elsevier.com/locate/heares

Upregulation of HSP by geranylgeranylacetone protects the cochlear lateral wall from endotoxin-induced inflammation

Michihiko Sone *, Hideo Hayashi, Hiroshi Yamamoto, Tatsuya Hoshino, Toru Mizushima, Tsutomu Nakashima

Department of Otorhinolaryngology, Nagoya University Graduate School of Medicine, 65 Tsurumai-cho, Showa-ku, Nagoya 466-8550, Japan
Department of Microbiology, Kumamoto University Graduate School of Medicine and Pharmaceutical Sciences, Kumamoto, Japan

Received 6 September 2004; accepted 22 January 2005
Available online 2 March 2005

Available online at www.sciencedirect.com
SCIENCE DIRECT®
Hearing Research 204 (2005) 140–146
HEARING RESEARCH
www.elsevier.com/locate/heares

Upregulation of HSP by geranylgeranylacetone protects the cochlear lateral wall from endotoxin-induced inflammation

Michihiko Sone *, Hideo Hayashi, Hiroshi Yamamoto, Tatsuya Hoshino, Toru Mizushima, Tsutomu Nakashima

Department of Otorhinolaryngology, Nagoya University Graduate School of Medicine, 65 Tsurumai-cho, Showa-ku, Nagoya 466-8550, Japan
Department of Microbiology, Kumamoto University Graduate School of Medicine and Pharmaceutical Sciences, Kumamoto, Japan

Received 6 September 2004; accepted 22 January 2005
Available online 2 March 2005

Abstract

We investigated whether an acyclic polyisoprenoid antiulcer drug, geranylgeranylacetone (GGA), induces the expression of HSP70 in the rat cochlea. Immunoblotting revealed upregulation of HSP70 in the cochlea at 12 h after transtympanic (local) or oral (systemic) administration of GGA, and this increased at 24 h after administration. Positive immunohistochemical staining of HSP70 was observed in the hair cells, the spiral ganglion, the stria vascularis, the spiral ligament, and the perivascular portion of modiolar vessels. We therefore subsequently studied the effects of GGA as an HSP-inducer on inner ear trauma due to inflammation. Damage to the lateral wall due to inflammation induced by lipopolysaccharide inoculation was protected against by pretreatment with GGA, as assessed physiologically by measurement of cochlear blood flow and morphologically by electron microscopy. The results of the present study suggest that GGA can protect the cochlea against other injuries including those induced by noise, ototoxic drugs, and ischemia by upregulating HSP70.

Keywords: GGA; HSP; Inner ear; Otitis media; Cochlear trauma

1. Introduction

The stress response represents a universally conserved cellular defense program. The best example of this increased cellular protection is the phenomenon of "acquired thermotolerance" (Minowada and Welch, 1995). Transient whole-body hyperthermia has been demonstrated to protect against cerebral ischemic cell damage in the rat (Chopp et al., 1989). Molecular chaperones are produced constitutively, and play a fundamental role in several important processes under normal, unstressed conditions (Minowada and Welch, 1995; Hayes and Dice, 1996). The intracellular accumulation of abnormally folded proteins initiates the stress response by activating heat-shock factors, which rapidly trimerize in response to metabolic stress. Trimerization enables heat-shock factors to bind to heat-shock elements, resulting in a high level of transcription of heat-shock genes. Heat-shock proteins (HSPs) bind to immature proteins and prevent premature and improper binding and folding.

The cochlea contains many mechanisms that are involved in the cellular response to stress (Altschuler et al., 2002). Sound conditioning is an active process induced by exposure to low-level, nondamaging noise that provides long-term protection against noise trauma (Niu and Canlon, 2002). HSPs can be induced in the inner ear by several stresses, including acoustic overstimulation

Abbreviations: GGA, geranylgeranylacetone; HSP, heat shock protein; LPS, lipopolysaccharide; INOS, inducible nitric oxide synthase; AICA, anterior inferior cerebellar artery; LD, laser-Doppler

* Corresponding author. Tel.: +81 52 744 2323; fax: +81 52 744 2325.
E-mail address: michsone@med.nagoya-u.ac.jp (M. Sone).

0378-5955/$ - see front matter © 2005 Elsevier B.V. All rights reserved.
doi:10.1016/j.heares.2005.01.012

(Lim et al., 1993), cisplatin (Oh et al., 2000), and hyperthermia (Fairfield et al., 2004), and sound-conditioning-induced HSP70 production was reported to protect the mouse cochlea from acoustic injury (Yoshida et al., 1999).

An acyclic polyisoprenoid antiulcer drug, geranylgeranylacetone (GGA), has been previously used to induce transcriptional activation of HSP70 genes, and reported to increase gastric mucosal defense systems (Hirakawa et al., 1996). The effects of GGA on HSP induction have been reported in other organs, including heart (Ooie et al., 2001), liver (Oda et al., 2002), and brain (Fujiki et al., 2003). Antiviral effects of GGA have also been reported (Unoshima et al., 2003). HSP70 families stabilize unfolded proteins prior to their assembly into multimolecular complexes, and associated genes are found in most cellular compartments (Becker and Craig, 1994).

The clinical implications of stress response have been indicated in infections, and HSP induction was also reported to inhibit inducible nitric oxide synthase (iNOS) and attenuate hypotension in endotoxin challenged rats (Hauser et al., 1996). We have previously reported that otitis media induces damage to the cochlear lateral wall, and the therapeutic effects of intratympanic administration of steroid and iNOS inhibitor (Sone et al., 2003, 2004). In this study, we investigated whether GGA induces the expression of HSP70 in the cochlea, and hence could prevent the damage to the cochlear lateral wall induced by inflammation.

2. Materials and methods

2.1. Animals and administration of GGA

We used 40 female Sprague–Dawley rats weighing 150–225 g. During surgery and when they were killed, the animals were anesthetized by the intramuscular injection of a mixture of ketamine hydrochloride (40 mg/kg), xylazine hydrochloride (8 mg/kg), and acepromazine maleate (1 mg/kg). All animals were free of middle ear infection prior to experiments. GGA was obtained from Eisai (Tokyo, Japan), and administered in two ways: systemically (oral) and locally (transtympanic).

2.2. Systemic administration

GGA, as an emulsion with 5% gum arabic and 0.008% tocopherol, was given orally at a dose of 800 mg/kg (2.4×10^{-3} M/kg) (systemic GGA group). As a control, rats were given the same dose of vehicle (systemic control group).

2.2.1. Local administration

Thirty microliters of GGA (5.0×10^{-4} M/kg) dissolved in absolute ethanol (final concentration of 1%) was given transtympanically into the middle ear cavity under a microscope (local GGA group). Ethanol is known to induce of HSP, and hence control rats were given 30 μl of 1% ethanol (local control group).

The treated animals were examined at 12 or 24 h after administration. After deep anesthesia, the inner ears of the rats were resected and examined. Experimental protocols were approved by the Nagoya University Committee on the Use and Care of Animals.

2.3. Immunoblotting

Cochleas (four ears in each group) were dissected and diluted in dissociation buffer, and then centrifuged. The total protein concentration of the cochleas was quantified by the Bradford method. An equal amount of total protein in each fraction was subjected to 8% SDS–PAGE and transferred electrophoretically to a polyvinylidene difluoride membrane. The membrane was incubated with antibodies against HSP70 (mouse monoclonal IgG; Stressgen Biotechnologies, Victoria, Canada) or actin (goat polyclonal IgG; Santa Cruz Biotechnology, CA, USA) overnight at 4 °C, and exposed to secondary antibodies of goat antimouse IgG-HRP (Amersham Biosciences, Buckinghamshire, UK) or mouse antigoat IgG-HRP (Santa Cruz Biotechnology) for 1 h at room temperature. The proteins were detected by enhanced chemiluminescence, and quantified using NIH imaging software.

2.4. Immunohistochemistry

Rat cochleas (four ears in each group) were removed and fixed with 4% paraformaldehyde. The tissues were then decalcified in 10% EDTA and embedded in paraffin. Blocks were sectioned at a thickness of 3 μm, and the sections were incubated with anti HSP70 antibody (mouse monoclonal IgG1; Stressgen Biotechnologies) as the primary antibody and biotinylated rabbit anti-mouse IgG (Dako, CA, USA) as the secondary antibody. Staining was performed with a Catalyzed Signal Amplification kit (Dako), which is an extremely sensitive immunohistochemical staining procedure incorporating signal-amplification methods based on the peroxidase-catalyzed deposition of a biotinylated phenoic compound. After incubation with streptavidin-peroxidase, sections were developed with diaminobenzidine tetrahydrochloride and hydrogen peroxide, and counterstained with hematoxylin. Sections without primary antibody treatment served as negative controls.

2.5. Pretreatment by GGA in rats with endotoxin-induced inflammation

To investigate the effects of GGA (as an inducer of HSP) on inner ear trauma caused by endotoxin-induced

inflammation in the middle ear, 800 mg/kg GGA was given orally 24 h before inflammation was induced. The preparation of the animal model with inflammation in the middle ear is described elsewhere (Sone et al., 2003, 2004). Briefly, endotoxin inoculation was performed by instilling lipopolysaccharide (LPS; 5 mg/ml) from *Escherichia coli* (Sigma, St. Louis, MO, USA) into the middle ear cavity of each animal. Control rats were given the same dose of vehicle 24 h before LPS-inoculation. Treated animals were examined at 24 h after LPS-inoculation. Each group consisted of four ears.

2.5.1. Measurement of cochlear blood flow and clamping of the anterior inferior cerebellar artery

The measurement technique used are described elsewhere (Yamamoto et al., 2003). Briefly, each bulla was opened carefully through a ventrolateral approach under general anesthesia. The 1.0-mm probe of a laser-Doppler (LD) flowmeter (ALF21, Advance, Tokyo, Japan) was placed over the basal turn of the cochlea, where maximum output of the device was obtained. The basilar artery and the anterior inferior cerebellar artery (AICA) were exposed by opening the dura, after which the AICA was occluded for 5 min by pressure from a metal stick with a 0.6-mm-diameter spherical tip. The cochlear blood flow and blood pressure were monitored continuously, using a computer-based chart recorder.

2.5.2. Electron microscopy

After deep anesthesia, the inner ears of the rats were resected and the lateral walls of cochlear basal turns were examined since, in a previous study, we found that the pathological changes were most prominent in the cochlear basal turn of rats after inoculation of LPS into the middle ear cavity. The inner ears were fixed by perilymphatic perfusion with a mixture of 2% paraformaldehyde and 2.5% glutaraldehyde, postfixed in 1% osmium, dehydrated, and embedded in Epon. Ultrathin sections of the cochlear lateral walls were stained with uranyl acetate and lead citrate, and examined using a Hitachi H-7100 transmission electron microscope.

2.6. Statistical analysis

Data were analyzed using the Kruskal–Wallis test and the Mann–Whitney test.

3. Results

3.1. Expression of HSP70 in the cochlea following administration of GGA

3.1.1. Immunoblotting

At 12 h after administration of GGA, upregulation of HSP70 was observed in the cochleas of both local (the density was 151% that of untreated rats) and systemic (relative density of 198%) GGA groups compared to normal rats, with a higher level of expression in the systemic group (Fig. 1). Upregulation was not observed in the cochleas 12 h after the local application of ethanol (local control group) (102%). HSP70 expression was increased in the cochleas 24 h after the local application of ethanol (relative density of 230%), but the expression was stronger in the cochleas of both local (relative density of 271%) and systemic (relative density of 254%) GGA groups. In each group, HSP expression was higher 24 h after administration than at 12 h. There was a tendency for the relative density of HSP70 to be more varied in rats of local groups than in those of systemic groups.

3.1.2. Immunohistochemistry

Compared with normal rats, stronger positive staining of HSP70 was observed in the cochleas of all GGA-treated groups, and at 24 h after the local application of ethanol (local control group). Positive staining was found in the cytoplasm of both inner and outer hair cells, supporting cells, the spiral limbus, the spiral ganglion cells, the stria vascularis, cells and connective tissue in the spiral ligament, and the perivascular portion of modiolar vessels (Fig. 2). Similar to the results obtained by immunoblotting, there was a tendency for the positive staining of HSP70 in the cochlea to be more varied in rats of local groups than in those of systemic groups. The expression of HSP70 in the lateral wall of animals of local groups was more prominent in the basal turn than in the apical turns.

Fig. 3 shows the expression of HSP70 in the lateral wall of animals in each group. Compared with normal rats, rats at 12 h after the local administration of ethanol or GGA showed stronger positive staining in the lateral

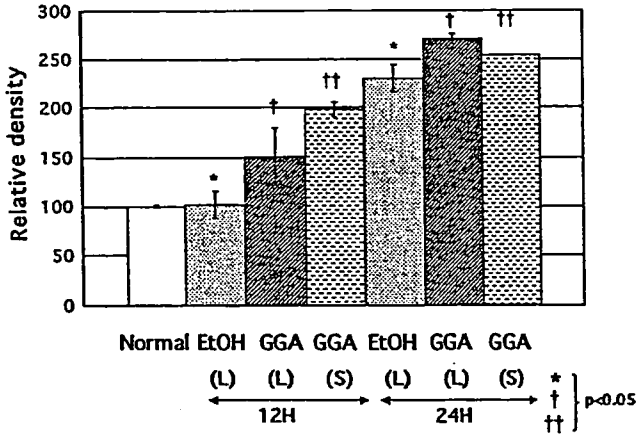

Fig. 1. Expression of HSP70 after local (L) treatment with ethanol (EtOH) or GGA, or systemic (S) treatment with GGA, as revealed by immunoblotting. Cochleas were investigated 12 h (12H) or 24 h (24H) after application. Data are the density relative to that of untreated rats (normal) (mean ± SE, $n = 4$ in each group).

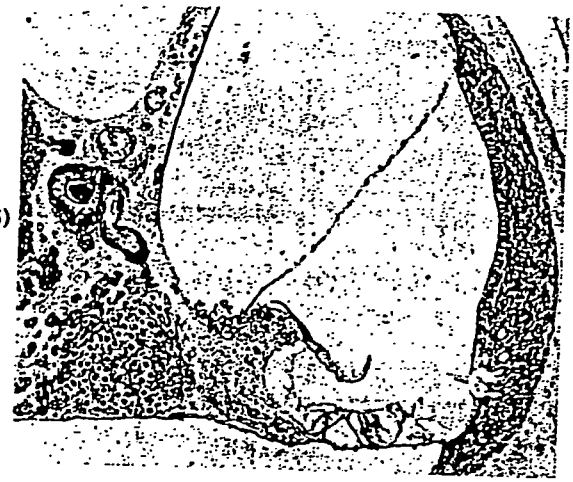

Fig. 2. Immunohistochemical staining with anti-HSP70 antibody after 24 h in the cochlea of a rat of the systemic GGA group. Strong expression of HSP70 is evident in the organ of Corti, the spiral ganglion, the stria vascularis, the spiral ligament, and the perivascular portion of modiolar vessels.

wall, and the strongest expression was found at 24 h in rats of the systemic GGA group. The cochleas of animals of vehicle groups were not different from normal groups.

3.2. Effects of pretreatment by GGA in rats with endotoxin-induced inflammation

3.2.1. Changes of cochlear blood flow on clamping and releasing of the AICA

The LD output dropped significantly (37–50%) after AICA clamping in both groups of rats. A prominent rebound in the blood flow after releasing the AICA was observed in rats pretreated with GGA before LPS-inoculation, compared with vehicle rats (Fig. 4).

3.2.2. Electron microscopy findings

The stria vascularis of vehicle rats showed very marked enlargement of the intercellular spaces in the intermediate cell area, and projection of the marginal cells towards the endolymphatic space was also observed (Fig. 5A). The stria vascularis of rats pretreated with GGA 24 h before LPS-inoculation appeared virtually normal (Fig. 5B). There were no abnormal findings in the spiral ligament of any rats.

4. Discussion

The stress response represents a universally conserved cellular defense mechanisms, as illustrated by the phenomenon of "acquired thermotolerance" (Minowada and Welch, 1995). Molecular chaperones are produced constitutively, and play a fundamental role in several important processes under normal, unstressed conditions (Minowada and Welch, 1995; Hayes and Dice, 1996). The functions include the promotion of correct protein folding after synthesis, stimulation of the assembly and disassembly of multimetric proteins, and facilitation of protein translocation. HSP70 families stabilize unfolded proteins prior to their assembly into multimolecular complexes, and these genes are found in most cellular compartments (Becker and Craig, 1994). The use of gene transfer to increase the levels of HSP70 was reported to reduce inflammation and injury in the hearts and the lungs of experimental animal models (Suzuki et al., 1997; Weiss et al., 2002).

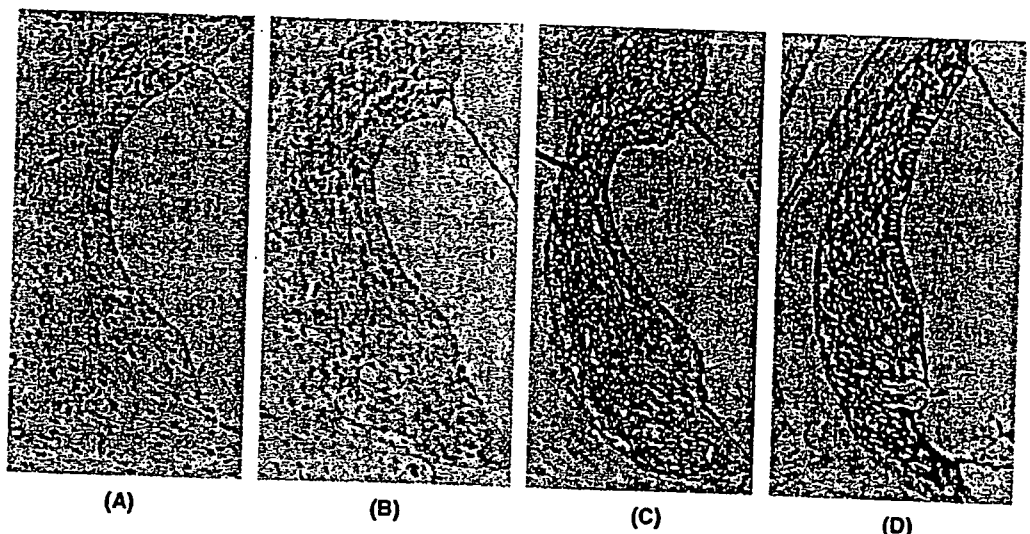

Fig. 3. Immunohistochemical staining with anti-HSP70 antibody in the lateral wall of a normal rat (A), rats 12 h after local administration with ethanol (B) or GGA (C), and a rat 24 h after the systemic administration of GGA (D). The strongest expression was found after 24 h in the rat of the systemic GGA group.

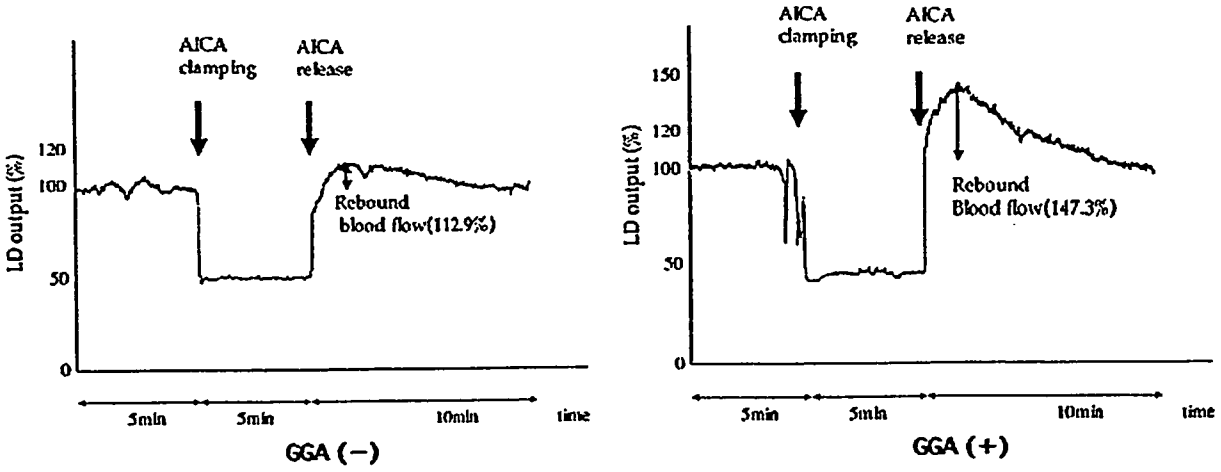

Fig. 4. Change in LD output following AICA clamping in a rat pretreated with GGA (GGA+) or a vehicle (GGA−) before LPS-inoculation. All values are expressed as percentage changes from the baseline value (BV).

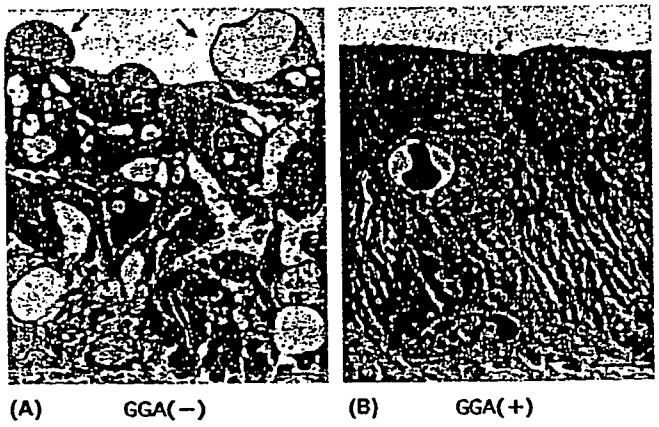

Fig. 5. Electron microscopy findings for the stria vascularis in rats pretreated with vehicle (GGA−) (A) or GGA (GGA+) (B). (A) Intercellular spaces in the intermediate cells are markedly enlarged (asterisks), and the marginal cells project towards the endolymphatic space (arrows). Scale bar = 2 μm. (B) The stria vascularis appears virtually normal. Scale bar = 2 μm.

GGA causes rapid activation of heat-shock factor and expression of HSP70 messenger RNA in cells (Hirakawa et al., 1996), although the exact mechanism has not been elucidated. The molecular weight of GGA is 330.5, and hence GGA can pass into the inner ear from the middle ear through the round window membrane (RWM). Although GGA is a nontoxic agent, local administration might still be a more effective therapy by further reducing possible side effects.

Immunoblotting revealed upregulation of HSP70 in the cochlea 12 h after the administration of GGA in both local and systemic groups, although the level was higher in the systemic group. At 24 h after GGA administration, the expression of HSP70 was higher in rats of the local group than in those of the systemic group, which may be attributable to the time it takes for locally applied GGA to reach the entire cochlea by passing through the RWM. For the concentrations of GGA used in the present study, local application was more effective than systemic application, although it should be dissolved in ethanol for local administration because of its oily nature, and the side effects of ethanol would need to be considered in clinical trials.

Immunohistochemically, positive staining of HSP70 was observed within the cochlea in all GGA-treated groups in hair cells and supporting cells of the organ of Corti, the spiral ganglion, the stria vascularis, the spiral ligament, and the perivascular portion of modiolar vessels. Similar to the immunoblotting results, there was a tendency for the HSP70 expression to be more varied among the rats of local groups compared to those of systemic groups. The expression of HSP70 in the lateral wall of animals of local groups was more prominent in the basal turn than in the apical turns, which may be attributable to their relative proximities to the RWM especially since this trend was not observed in the lateral walls of the systemic groups. The strongest expression of HSP70 in the lateral wall was found after 24 h in the rat of the systemic GGA group. Quantification of immunohistochemistry images showed that the strength of HSP70 expression in rats 12 h after the local administration of ethanol or GGA, and in rats 24 h after the systemic administration of GGA, was 3.9, 19.3, and 40.0 times greater than that in normal rats, respectively (data not shown).

Upregulation of HSP in the rat cochlea after acoustic overstimulation (Lim et al., 1993) or hyperthermia (Fairfield et al., 2004) has been observed in the outer hair cells and the stria vascularis, but not in the inner hair cells, the spiral ligament, or the spiral ganglion cells (Lim et al., 1993). The differences in the underlying mechanisms between these previous studies and our present results are unclear. Trauma is considered to stimulate the upregulation of HSP in some regions, whereas GGA may induce HSP without traumatic stimulation.

There is a possibility that the administration itself induces the stress response. However, in a preliminary study, we immunohistochemically checked the expression of HSP in the cochlea of animals that received phosphate-buffered saline in the right middle ear cavity, and found no such upregulation.

After single-dose administration of GGA, mRNA expression of HSP in the brain was observed from 4 h then slowly decreased, and disappeared by 48 h (Nikaido et al., 2004). Western immunoblotting analysis in the rat heart revealed that HSP was present from 6 h and peaked at 24 h after GGA administration (Ooie et al., 2001). As shown in the present study, the effect of protection by HSP in the cochlea against trauma may also peak at 24 h after GGA administration.

Inner ear disorders caused by inflammation in the middle ear that are not treated early could lead to permanent inner ear damage. HSP has been considered to protect cells during inflammation associated with the toxicity of nitric oxide (Jacquier-Sarlin et al., 1994). A study using an HSP-inducer, sodium arsenite, demonstrated that the expression of HSP protected against iNOS expression and attenuated hypotension in rats treated with LPS (Hauser et al., 1996). Other studies have also shown that members of the HSP70 family inhibited iNOS expression (Matsuda et al., 2000; Dobbin et al., 2002). The upregulation of HSP70 in the cochlea following GGA administration, as seen in the present study, prompted us to also investigate whether GGA protects the cochlear lateral wall from damage induced by inflammation.

The rebound effect we observed after the release of AICA clamping is thought to reflect the autoregulation of blood flow in the inner ear (Yamamoto et al., 2003). This finding demonstrates physiologically that GGA can protect the lateral wall from damage induced by LPS-inoculation. The result was confirmed morphologically by electron microscopy, which revealed that the appearance of the stria vascularis was virtually normal in rats pretreated with GGA. GGA itself might influence iNOS expression in the cochlea, but oral administration of GGA was shown not to induce iNOS in rat hearts (Ooie et al., 2001). Antiapoptotic effects following GGA administration have been reported in the liver (Ikeyama et al., 2001), and the cochlear lateral walls in the present study might be partially protected by this mechanism.

GGA administration induced HSP70 in hair cells and supporting cells of the organ of Corti, the spiral ganglion, and the perivascular portion of modiolar vessels, as well as in the lateral wall. These findings suggest that GGA protects the cochlea against other injuries to these target structures through the upregulation of HSP70, such as induced by noise, ototoxic drugs, and ischemia. GGA might induce other HSPs in the cochlea besides HSP70, suggesting the prophylactic use of this drug in clinical applications.

Acknowledgement

This work was supported in part by research grants from the Ministry of Education, Culture, Sports, Science and Technology of the Japanese Government.

References

Altschuler, R.A., Fairfield, D., Cho, Y., Leonova, E., Benjamin, I.J., Miller, J.M., Lomax, M.I., 2002. Stress pathways in the rat cochlea and potential for protection from acquired deafness. Audiol. Neurootol. 7, 152–156.

Becker, J., Craig, E.A., 1994. Heat-shock proteins as molecular chaperones. Eur. J. Biochem. 219, 11–13.

Chopp, M., Chen, H., Ho, K.-L., Dereski, M.O., Brown, E., Hetzel, F.W., Welch, K.M.A., 1989. Transient hyperthermia protects against subsequent forebrain ischemic cell damage in the rat. Neurology 39, 1396–1398.

Dobbin, C.A., Smith, N.C., Johnson, A.M., 2002. Heat shock protein 70 is a potential virulence factor in murine toxoplasma infection via immunomodulation of host NF-κB and nitric oxide. J. Immunol. 169, 958–965.

Fairfield, D.A., Kanicki, A.C., Lomax, M.I., Altschuler, R.A., 2004. Induction of heat shock protein 32 (HSP32) in the rat cochlea following hyperthermia. Hear. Res. 188, 1–11.

Fujiki, M., Kobayashi, H., Abe, T., Ishi, K., 2003. Astroglial activation accompanies heat shock proteins upregulation in rat brain following single oral dose of geranylgeranylacetone. Brain Res. 991, 254–257.

Hauser, G.J., Dayao, E.K., Wasserloos, K., Pitt, B.R., Wong, H.R., 1996. HSP induction inhibits iNOS mRNA expression and attenuates hypotension in endotoxin-challenged rats. Am. J. Physiol. 271, H2529–H2535.

Hayes, S.A., Dice, J.F., 1996. Roles of Molecular chaperones in protein degradation. J. Cell. Biol. 132, 255–258.

Hirakawa, T., Rokutan, K., Nikawa, T., Kishi, K., 1996. Geranylgeranylacetone induces heat shock proteins in cultured guinea pig gastric mucosal cells and rat gastric mucosa. Gastroenterology 111, 354–357.

Ikeyama, S., Kusumoto, K., Miyake, H., Rokutan, K., Tashiro, S., 2001. A non-toxic heat shock protein 70 inducer, geranylgeranylacetone, suppresses apoptosis of cultured rat hepatocytes caused by hydrogen peroxide and ethanol. J. Hepatol. 35, 53–61.

Jacquier-Sarlin, M.R., Fuller, K., Dinh-Xuan, A.T., Richard, M.J., Polla, B.S., 1994. Protective effects of hsp70 in inflammation. Experientia 50, 1031–1038.

Lim, H.H., Jenkins, O.H., Myers, M.W., Miller, J.M., Altschuler, R.A., 1993. Detection of HSP 72 synthesis after acoustic overstimulation in rat cochlea. Hear. Res. 69, 146–150.

Matsuda, H., Kagerura, T., Toguchida, I., Ueda, H., Morikawa, T., Yoshikawa, M., 2000. Inhibitory effects of sesquiterpenes from bay leaf on nitric oxide production in lipopolysaccharide-activated macrophages: structure requirement and role of heat shock protein induction. Life Sci. 66, 2151–2157.

Minowada, G., Welch, W.J., 1995. Clinical implications of the stress response. J. Clin. Invest. 95, 3–12.

Niu, X., Canlon, B., 2002. Protective mechanisms of sound conditioning. Adv. Otorhinolaryngol. 59, 96–105.

Nikaido, H., Tsunoda, H., Nishimura, Y., Kirino, T., Tanaka, T., 2004. Potential role for heat shock protein 72 in antagonizing cerebral vasospasm after rat subarachnoid hemorrhage. Circulation 110, 1839–1846.

Oda, H., Miyake, H., Iwata, T., Kusumoto, K., Rokutan, K., Tashiro, S., 2002. Geranylgeranylacetone suppresses inflammatory

responses and improves survival after massive hepatectomy in rats. J. Gastrointest. Surg. 6, 464–473.

Oh, S.H., Yu, W.S., Song, B.H., Lim, D., Koo, J.W., Chang, S.O., Kim, C.S., 2000. Expression of heat shock protein 72 in rat cochlea with cisplatin-induced acute ototoxicity. Acta Otolaryngol. 120, 146–150.

Ooie, T., Takahashi, N., Saikawa, T., Nawata, T., Arikawa, M., Yamanaka, K., Hara, M., Shimada, T., Sakata, T., 2001. Single oral dose of geranylgeranylacetone induces heat-shock protein 72 and renders protection against ischemia/reperfusion injury in rat heart. Circulation 104, 1837–1843.

Sone, M., Hayashi, H., Yamamoto, H., Tominaga, M., Nakashima, T., 2003. A comparative study of intratympanic steroid and NO synthase inhibitor for treatment of cochlear lateral wall damage due to acute otitis media. Eur. J. Pharmacol. 482, 313–318.

Sone, M., Hayashi, H., Tominaga, M., Nakashima, T., 2004. Changes of cochlear blood flow due to endotoxin-induced otitis media. Ann. Otol. Rhinol. Laryngol. 113, 450–454.

Suzuki, K., Sawa, Y., Kaneda, Y., Ichikawa, H., Shirakura, R., Matsuda, H., 1997. In vivo gene transfection with heat shock protein 70 enhances myocardial tolerance to ischemia-reperfusion injury in rat. J. Clin. Invest. 99, 1645–1650.

Unoshima, M., Iwasaka, H., Eto, J., Takita-Sonoda, Y., Noguchi, T., Nishizono, A., 2003. Antiviral effects of geranylgeranylacetone: enhancement of $M \times A$ expression and phosphorylation of PKR during influenza infection. Antimicrob. Agents Chemother. 47, 2914–2921.

Yamamoto, H., Tominaga, M., Sone, M., Nakashima, T., 2003. Contribution of stapedial artery to blood flow in the cochlea and its surrounding bone. Hear. Res 186.

Yoshida, N., Kristiansen, A., Liberman, M.C., 1999. Heat stress and protection from permanent acoustic injury in mice. J. Neurosci. 19, 10116–10124.

Weiss, Y.G., Maloyan, A., Tazelaar, J., Raj, N., Deutschman, C.S., 2002. Adenoviral transfer of HSP-70 into pulmonary epithelium ameliorates experimental acute respiratory distress syndrome. J. Clin. Invest. 110, 801–806.

THE JOURNAL OF BIOLOGICAL CHEMISTRY

Vol. 280, No. 35, Issue of September 2, pp. 31059–31067, 200
Printed in U.S.A

Involvement of Intracellular Ca^{2+} Levels in Nonsteroidal Anti-inflammatory Drug-induced Apoptosis*

Received for publication, March 17, 2005, and in revised form, May 25, 2005
Published, JBC Papers in Press, June 29, 2005, DOI 10.1074/jbc.M502956200

Ken-ichiro Tanaka‡, Wataru Tomisato‡, Tatsuya Hoshino‡, Tomoaki Ishihara‡, Takushi Namba‡, Mayuko Aburaya‡, Takashi Katsu§, Keitarou Suzuki‡, Shinji Tsutsumi‡, and Tohru Mizushima‡¶

From the ‡Graduate School of Medical and Pharmaceutical Sciences, Kumamoto University, Kumamoto 862-0973, and the §Faculty of Pharmaceutical Sciences, Okayama University, Okayama 700-8530, Japan

We recently reported that nonsteroidal anti-inflammatory drug (NSAID)-induced gastric lesions involve NSAID-induced apoptosis of gastric mucosal cells, which in turn involves the endoplasmic reticulum stress response, in particular the up-regulation of CCAAT/enhancer-binding protein homologous transcription factor (CHOP). In this study, we have examined the molecular mechanism governing this NSAID-induced apoptosis in primary cultures of gastric mucosal cells. Various NSAIDs showed membrane permeabilization activity that correlated with their apoptosis-inducing activity. Various NSAIDs, particularly celecoxib, also increased intracellular Ca^{2+} levels. This increase was accompanied by K^+ efflux from cells and was virtually absent when extracellular Ca^{2+} had been depleted. These data indicate that the increase in intracellular Ca^{2+} levels that is observed in the presence of NSAIDs is due to the stimulation of Ca^{2+} influx across the cytoplasmic membrane, which results from their membrane permeabilization activity. An intracellular Ca^{2+} chelator partially inhibited celecoxib-induced release of cytochrome *c* from mitochondria, reduced the magnitude of the celecoxib-induced decrease in mitochondrial membrane potential and inhibited celecoxib-induced apoptotic cell death. It is therefore likely that an increase in intracellular Ca^{2+} levels is involved in celecoxib-induced mitochondrial dysfunction and the resulting apoptosis. An inhibitor of calpain, a Ca^{2+}-dependent cysteine protease, partially suppressed mitochondrial dysfunction and apoptosis in the presence of celecoxib. Celecoxib-dependent CHOP-induction was partially inhibited by the intracellular Ca^{2+} chelator but not by the calpain inhibitor. These results suggest that Ca^{2+}-stimulated calpain activity and CHOP expression play important roles in celecoxib-induced apoptosis in gastric mucosal cells.

Nonsteroidal anti-inflammatory drugs (NSAIDs)[1] account for nearly 5% of all prescribed medications (1). The anti-inflammatory action of NSAIDs is mediated through their inhibitory effect on cyclooxygenase (COX) activity. COX is an enzyme essential for the synthesis of prostaglandins (PGs), which have a strong capacity to induce inflammation. On the other hand, NSAID use is associated with gastrointestinal complications (2), with about 15–30% of chronic users of NSAIDs suffering from gastrointestinal ulcers and bleeding (3–6).

The inhibition of COX by NSAIDs at gastrointestinal mucosa was previously thought to be the sole explanation for the gastrointestinal side effects of NSAIDs because PGs have a strong protective effect on gastrointestinal mucosa (7, 8). However, now it is believed that the induction of gastrointestinal lesions by NSAIDs involves additional mechanisms, since the increased incidence of gastrointestinal lesions and the decrease in PG levels induced by NSAIDs do not always occur in parallel (9, 10). We have previously demonstrated that NSAIDs induce cell death (apoptosis and necrosis) in primary cultures of gastric mucosal cells in a manner independent of COX inhibition (11, 12). Furthermore, we recently suggested that both COX inhibition and NSAID-induced cell death at gastric mucosa are required for NSAID-induced gastric lesions *in vivo* (12). Therefore, elucidation of the mechanisms governing NSAID-induced cell death is important for understanding the mechanisms by which NSAIDs cause gastric lesions and may allow the development of new safer NSAIDs. We recently showed that all of the NSAIDs tested have membrane permeabilization activity, which is implicated in NSAID-induced apoptosis and necrosis (13). However, the mechanism by which the membrane permeabilization activity of NSAIDs causes cell death and in particular apoptosis in gastric mucosal cells remains unknown.

Accumulation of unfolded protein in the endoplasmic reticulum (ER) induces the ER stress response, otherwise known as the unfolded protein response. Cells initially adapt to the accumulation of unfolded proteins by inducing the expression of ER-resident molecular chaperones such as glucose-regulated protein 78 (14–17). However, if this adaptation does not prove sufficient, the apoptotic response is initiated, which is primarily the induction of the CCAAT/enhancer-binding protein homologous transcription factor (CHOP) (18). We recently reported that various NSAIDs induce not only glucose-regulated protein 78 but also CHOP expression. In addition to this, we showed, using CHOP-

* This work was supported by grants-in-aid for scientific research from the Ministry of Health, Labour, and Welfare of Japan as well as by the Suzuken Memorial Foundation, the Tokyo Biochemical Research Foundation, the Kumamoto Technology and Industry Foundation, and the Japan Research Foundation for Clinical Pharmacology. The costs of publication of this article were defrayed in part by the payment of page charges. This article must therefore be hereby marked "*advertisement*" in accordance with 18 U.S.C. Section 1734 solely to indicate this fact.

¶ To whom correspondence should be addressed: Graduate School of Medical and Pharmaceutical Sciences, Kumamoto University, Kumamoto 862-0973, Japan. Tel./Fax: 81-96-371-4323; E-mail: mizu@gpo.kumamoto-u.ac.jp.

[1] The abbreviations used are: NSAIDs, nonsteroidal anti-inflammatory drugs; COX, cyclooxygenase; PG, prostaglandin; PGE_2, prostaglandin E_2; ER, endoplasmic reticulum; CHOP, CCAAT/enhancer-binding protein homologous transcription factor; SERCA, sarcoendoplasmic reticulum Ca^{2+}-ATPase; BAPTA-AM, 1,2-bis(2-aminophenoxy)ethane-*N*,*N*,*N*′*N*′-tetraacetic acid; Ho 342, Hoechst 33342; MTT, 3-(4,5-dimethylthiazol-2-yl)-2,5-diphenyltetrazolium bromide; DePsipher, 5,5′,6,6′-tetrachloro-1, 1′,3,3′-tetraethylbenzimidaozolylcarbocyanine iodide; Z-Leu-Leu-H, carbobenzoxy-L-leucyl-L-leucinal; AMC, aminomethylcoumarin; PIPES, 1,4-piperazinediethanesulfonic acid; CHAPS, 3-[(3-cholamidopropyl)dimethylammonio]-1-propanesulfonic acid.

deficient mice and a dominant negative form of CHOP, that this CHOP induction is essential for NSAID-induced apoptosis (19). Therefore, NSAIDs seem to induce apoptosis by acting as ER stressors. However, the mechanism by which NSAIDs induce the ER stress response has remained unknown. Other groups have pointed out the involvement of mitochondrial dysfunction in NSAID-induced apoptosis; some NSAIDs (such as celecoxib) stimulate the release of cytochrome *c* from mitochondria and decrease the mitochondrial membrane potential (20, 21). Various mechanisms have been proposed for NSAID-induced mitochondrial dysfunction, such as inactivation of phosphatidylinositol 3-kinase/3-phosphoinositide-dependent kinase-1/Akt or mitogen-activated protein kinase/extracellular signal-regulated kinase (20–22). However, data in these studies have some contradictions (may be due to differences in cell species), and the mechanisms by which NSAIDs cause mitochondrial dysfunction have also not been fully characterized.

Increases in intracellular Ca^{2+} levels, due to cellular Ca^{2+} overload or perturbation of intracellular Ca^{2+} compartmentalization, trigger apoptosis. For example, many apoptotic stimuli, such as activation of surface antigen receptors, increase the intracellular Ca^{2+} level, and compounds that directly increase the intracellular Ca^{2+} level (Ca^{2+} ionophores and inhibitors for sarcoendoplasmic reticulum Ca^{2+} ATPase (SERCA)) have been shown to induce apoptosis (23–25). Various mechanisms have been proposed for the Ca^{2+}-induced apoptosis pathway, such as activation of protein kinase C, opening of permeability transition pores in mitochondria, and stimulation of reactive oxygen species synthesis (26–29). In addition, calpain, a Ca^{2+}-dependent cysteine protease, plays an important role in the Ca^{2+}-induced apoptosis pathway. Calpain activates or inhibits Bax and Bid or Bcl-2 and Bcl-X_L, respectively, by their cleavage, resulting in stimulation of the release of cytochrome *c* from mitochondria and a decrease in the mitochondrial membrane potential. Then cytochrome *c* activates caspase-9, which in turn activates caspase-3 and induces apoptosis. It is also suggested that calpain directly activates some caspases (26, 29–32). On the other hand, recent reports show that Ca^{2+} ionophores induce the ER stress response and CHOP expression, suggesting that increases in the intracellular Ca^{2+} level can induce the ER stress response and CHOP expression (26, 33).

Permeabilization of cytoplasmic membranes causes an increase in intracellular Ca^{2+} levels by stimulating Ca^{2+} influx across the cytoplasmic membrane. Some NSAIDs were shown to increase intracellular Ca^{2+} levels (13, 34). Therefore, it is reasonable to speculate that increases in intracellular Ca^{2+} levels are involved in NSAID-induced apoptosis (*i.e.* that the increased intracellular Ca^{2+} level connects the membrane permeabilization and CHOP induction activities of NSAIDs). Furthermore, it is also possible that activation of calpain connects the increases in intracellular Ca^{2+} levels to mitochondrial dysfunction in the presence of NSAIDs. In this study, we showed, in primary cultures of guinea pig gastric mucosal cells, that all NSAIDs tested increased intracellular Ca^{2+} levels, which accompanied the induction of apoptosis. An intracellular Ca^{2+} chelator partially inhibited CHOP induction, release of cytochrome *c* from mitochondria, the decrease in mitochondrial membrane potential, and apoptotic cell death in the presence of celecoxib (the most potent NSAID for apoptosis induction). Furthermore, an inhibitor of calpain partially suppressed the mitochondrial dysfunction and apoptotic cell death but did not affect CHOP induction in the presence of celecoxib. These results suggest that the celecoxib-dependent increase in intracellular Ca^{2+} levels and the resulting calpain activation and CHOP induction are involved in celecoxib-induced apoptosis in gastric mucosal cells.

EXPERIMENTAL PROCEDURES

Chemicals, Media, and Animals—Fetal bovine serum was from Invitrogen. RPMI 1640 and Hanks' solution were obtained from Nissui Pharmaceutical Co. Pronase E and type I collagenase were purchased from Kaken Pharmaceutical Co. and Nitta Gelatin Co., respectively. Pluronic F127, fluo-3/AM, 1,2-bis(2-aminophenoxy)ethane-*N*,*N*,*N*′,*N*′-tetraacetic acid (BAPTA-AM), and BAPTA were from Dojindo Co. Nimesulide and flurbiprofen were from Cayman Chemical Co. Indomethacin was from Wako Co. Hoechst 33342 (Ho 342), ibuprofen, diclofenac, 3-(4,5-dimethylthiazol-2-yl)-2,5-diphenyltetrazolium bromide (MTT), mefenamic acid, ketoprofen, and flufenamic acid were from Sigma. 5,5′,6,6′-tetrachloro-1,1′,3,3′-tetraethylbenzimidaozolylcarbocyanine iodide (DePsipher) was from Trevigen. Celecoxib was from LKT Laboratories Inc. Etodolac was a gift kindly provided by Nippon Shinyaku Co. Peptides for the assay of caspase-3 or calpain and carbobenzoxy-L-leucyl-L-leucinal (Z-Leu-Leu-H) were from Peptide Institute, Inc. Egg phosphatidylcholine was from Kanto Chemicals Co. Antibodies against CHOP and actin were from Santa Cruz Biotechnology Inc. Antibody against cytochrome *c* was from PharMingen. Male guinea pigs weighing 200–300 g were purchased from Kyudo Co. The experiments and procedures described here were carried out in accordance with the Guide for the Care and Use of Laboratory Animals as adopted and promulgated by the National Institutes of Health and were approved by the Animal Care Committee of Kumamoto University.

In Vitro Assay of Cytotoxicity—Gastric mucosal cells were isolated from guinea pig fundic glands as described previously (35). Isolated gastric mucosal cells were cultured for 12 h in RPMI 1640 containing 0.3% (v/v) fetal bovine serum, 100 units/ml penicillin, and 100 μg/ml streptomycin in type I collagen-coated plastic culture plates under conditions of 5% CO_2, 95% air and 37 °C. Nonadherent cells were removed, and the cells attached to the plate were used in the experiments. Guinea pig gastric mucosal cells prepared under these conditions have previously been characterized, with the majority (about 90%) of cells identified as pit cells (35).

NSAIDs were dissolved in Me_2SO or Na_2CO_3 (for indomethacin only) and control experiments (without NSAIDs) were performed in the presence of the same concentrations of Me_2SO or Na_2CO_3. Cells were exposed to NSAIDs by changing the medium. Cell viability was determined by the MTT method.

Apoptotic chromatin condensation was monitored as described previously (36). Cells were washed with PBS, stained with 10 μg/ml Ho 342, and observed under a fluorescence microscope.

Immunoblotting Analysis—Whole cell extracts were prepared as described previously (36). The protein concentration of the samples was determined by the Bradford method. The samples were electrophoresed on polyacrylamide gels containing SDS, and the proteins were then transferred to membranes and detected using antibodies.

Mitochondrial Membrane Potential Assay—Mitochondrial membrane potential was assayed using a fluorometric mitochondrial permeability assay kit (Trevigen) (36). Briefly, after treatment with NSAIDs, cells were treated with DePsipher (5 μg/ml) for 20 min at 37 °C and observed under a fluorescence microscope using 590 nm for red emission and 530 nm for green emission.

Measurement of the Intracellular Ca^{2+} Level—Intracellular Ca^{2+} levels were monitored as described (37). The cells were washed with assay buffer (115 mM NaCl, 5.4 mM KCl, 1.8 mM $CaCl_2$, 0.8 mM $MgCl_2$, 20 mM HEPES, and 13.8 mM glucose). For Ca^{2+}-free conditions, the modified assay buffer (115 mM NaCl, 5.4 mM KCl, 5 mM EGTA, 20 mM HEPES, and 13.8 mM glucose) was used instead of the normal assay buffer. The cells were then incubated with 4 μM fluo-3/AM in assay buffer supplemented with 0.1% bovine serum albumin, 0.04% pluronic F127, and 2 mM probenecid, for 40 min at 37 °C. After washing twice with assay buffer, cells were suspended in assay buffer supplemented with 2 mM probenecid. Cells were transferred to a water-jacketed cuvette (1.6×10^6 cells/cuvette), and the fluo-3 fluorescence was then measured with a Hitachi F-4500 spectrofluorophotometer by recording excitation signals at 490 nm and the emission signal at 530 nm at 1-s intervals. Maximum and minimum fluorescence values (F_{max} and F_{min}) were obtained by adding 10 μM ionomycin and 10 μM ionomycin under Ca^{2+}-free conditions, respectively. The intracellular Ca^{2+} level was calculated according to the equation, $[Ca^{2+}]_i = K_d(F - F_{min})/(F_{max} - F)$, where K_d is the apparent dissociation constant (400 nM) of the fluorescent dye-Ca^{2+} complex.

Membrane Permeability Assay—Permeabilization of calcein-loaded liposomes was assayed as described previously (13). Liposomes were prepared using the reversed-phase evaporation method. Egg phosphatidylcholine (10 μmol, 7.7 mg) was dissolved in chloroform/methanol (1:2,

v/v), dried, dissolved in 1.5 ml of diethyl ether, and added to 1 ml of 100 mM calcein-NaOH (pH 7.4). The mixture was sonicated to obtain a homogenous emulsion. The diethyl ether solvent was removed, and the resulting suspension of liposomes was centrifuged and washed twice with fresh buffer A (10 mM potassium buffer, containing 150 mM NaCl) to remove untrapped calcein. The final liposome precipitate was resuspended in 5 ml of buffer A. A 0.3-ml aliquot of this suspension was diluted with 19.7 ml of buffer A, and 400 μl of this diluted suspension was then incubated at 30 °C for 10 min in the presence of the NSAID under investigation. The release of calcein from liposomes was determined by measuring fluorescence intensity at 520 nm (excitation at 490 nm).

Assay for K^+ Efflux from Cells—K^+ efflux from cells was monitored as described previously (38) with some modifications. Cells were washed twice with buffer A and then suspended in fresh buffer A (6×10^6 cells/ml). After incubation with NSAIDs for 30 min at 37 °C, K^+ efflux from cells was measured with a K^+ ion-selective electrode.

Assay for Caspase Activity—The activity of caspase-3 was determined as described previously (36). Briefly, cells were collected by centrifugation and suspended in extraction buffer (50 mM PIPES (pH 7.0), 50 mM KCl, 5 mM EGTA, 2 mM $MgCl_2$, and 1 mM dithiothreitol). Suspensions were sonicated and centrifuged, after which the supernatants were incubated with fluorogenic peptide substrates (acetyl-DEVD-methylcoumarin amide) in reaction buffer (100 mM HEPES-KOH (pH 7.5), 10% sucrose, 0.1% CHAPS, and 1 mg/ml bovine serum albumin) for 15 min at 37 °C. The release of aminomethylcoumarin (AMC) was determined using a fluorescence spectrophotometer. One unit of protease activity was defined as the amount of enzyme required to release 1 pmol of AMC/min.

Assay for Calpain Activity—The activity of calpain was determined as described previously (30). Briefly, cells were collected by centrifugation, washed by Hanks' solution, and suspended with the same solution at 2.5×10^5 cells/ml. Suspensions were incubated with fluorogenic peptide substrates succinyl-L-leucyl-L-leucyl-L-valyl-L-tyrosine 4-methylcoumaryl-7-amide for 3 min at 37 °C. The release of AMC was determined using a fluorescence spectrophotometer.

Statistical Analyses—All values are expressed as the means ± S.E. One-way analysis of variance, followed by Scheffe's multiple comparison, was used for evaluation of differences between the groups. Student's *t* test for unpaired results was performed to evaluate differences between two groups. Differences were considered to be significant for values of $p < 0.05$.

RESULTS

Close Relationship between NSAID-induced Apoptosis and Membrane Permeabilization—We recently reported that some NSAIDs (celecoxib, mefenamic acid, flufenamic acid, nimesulide, and flurbiprofen) cause not only apoptosis in primary cultures of guinea pig gastric mucosal cells but also membrane permeabilization in calcein-loaded liposomes (13). To examine the relationship between the apoptosis-inducing and membrane permeabilization activities of NSAIDs, in this study, we have examined these activities of other NSAIDs. As shown in Fig. 1A, treatment of primary cultures of guinea pig gastric mucosal cells with celecoxib for 16 h decreased cell viability in a dose-dependent manner, and this is consistent with our previous results (13). Each of the NSAIDs tested here (indomethacin, diclofenac, etodolac, ibuprofen, and ketoprofen) also decreased cell viability in a dose-dependent manner. Because cell death under these conditions was accompanied by apoptotic DNA fragmentation and chromatin condensation (data not shown), it is most likely mediated by apoptosis.

Two subtypes of COX, COX-1 and COX-2, are responsible for the majority of COX activity in gastric mucosal and inflammatory tissues, respectively, and recently a number of COX-2-selective NSAIDs have been developed (39). Among the NSAIDs tested in Fig. 1A, etodolac and celecoxib have selectivity for COX-2. No relationship was evident between NSAID-induced apoptosis and selectivity for COX-2 (Fig. 1A). We also confirmed that exogenously added PGE_2 (either native PGE_2 or 16,16-dimethyl-PGE_2) did not affect NSAID-induced apoptosis even at a higher concentration of PGE_2 in the culture medium than is present endogenously (10^{-9} M) (data not shown). These

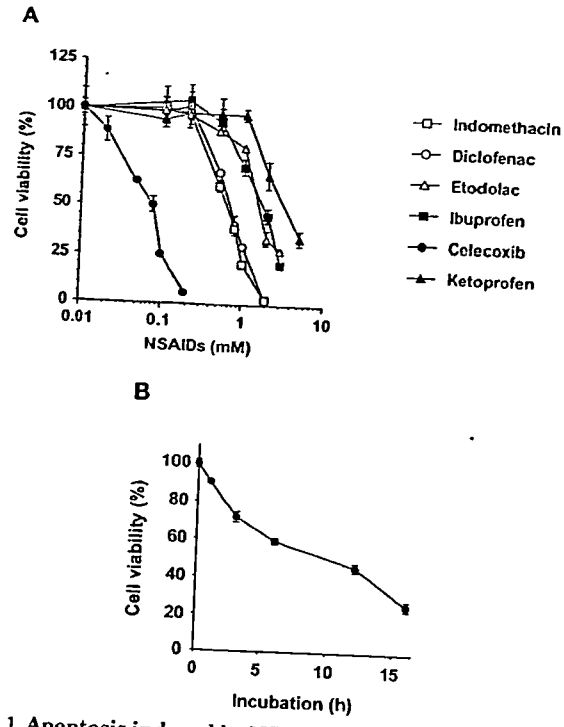

FIG. 1. **Apoptosis induced by NSAIDs.** Cultured guinea pig gastric mucosal cells were incubated with the indicated concentrations of each NSAID for 16 h (*A*) or with 100 μM celecoxib for the indicated periods (*B*). Cell viability was determined by the MTT method. Values are mean ± S.E. ($n = 3$).

data show that NSAID-induced apoptosis is independent of COX-inhibition by NSAIDs and are consistent with our previous conclusion (12, 13).

Calcein fluoresces very weakly at high concentrations due to self-quenching, so the addition of membrane-permeabilizing drugs to a medium containing calcein-loaded liposomes should cause an increase in fluorescence by diluting out the calcein (13). As shown in Fig. 2A, not only celecoxib but also other NSAIDs increased the calcein fluorescence, suggesting that they have membrane permeabilization activity.

Combining the results from the previous (13) and present studies, we obtained dose-response curves of 10 different NSAIDs for both induction of apoptosis and membrane permeabilization. To examine the relationship between NSAID-induced apoptosis and membrane permeabilization, we determined ED_{50} values of the 10 NSAIDs for apoptosis (concentrations of NSAIDs required for 50% inhibition of cell viability by apoptosis) and ED_{20} values for membrane permeabilization (concentration of NSAIDs required for 20% release of calcein) (Table I). We used ED_{20} values instead of ED_{50} values for estimating the activity of each NSAID for membrane permeabilization, because ED_{50} values of etodolac for calcein release could not to be determined (Fig. 2A). Plotting ED_{50} values for apoptosis *versus* ED_{20} values for membrane permeabilization (calcein release) yielded an r^2 value of 0.929 (Fig. 3A), which suggests that NSAID-induced apoptosis is mediated by their ability to permeabilize membranes.

Mechanism whereby the Intracellular Ca^{2+} Level Is Increased by NSAIDs—Fig. 4A shows the effect of various NSAIDs on the intracellular Ca^{2+} level. Not only celecoxib but also all of the other NSAIDs tested increased the intracellular Ca^{2+} level in a dose-dependent manner. Since indomethacin absorbs fluo-3 fluorescence (530 nm), we could not measure the intracellular Ca^{2+} level in the presence of indomethacin by this assay system. In order to estimate the activity of each NSAID for Ca^{2+} increase, we determined the concentration of each

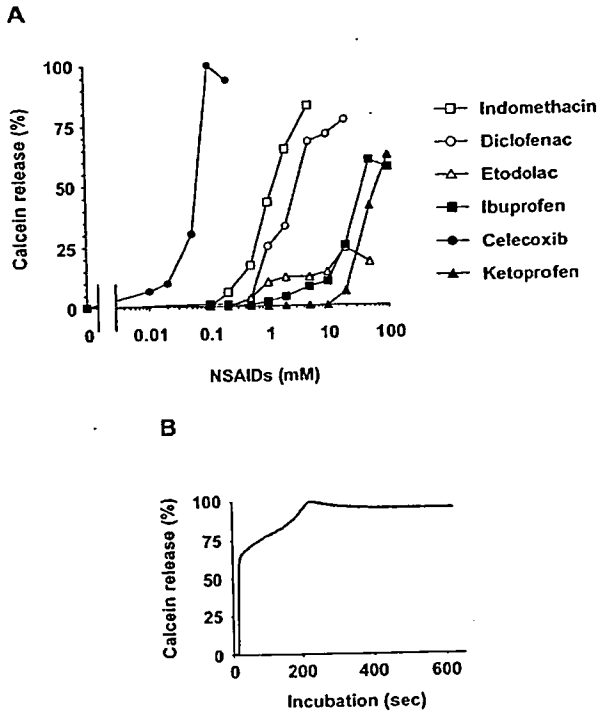

FIG. 2. **Membrane permeabilization by NSAIDs.** Calcein-loaded liposomes were incubated for 10 min with the indicated concentrations of each NSAID (*A*) or with 100 μM celecoxib for the indicated periods (*B*). The release of calcein from liposomes was determined by measuring fluorescence intensity. Melittin (10 μM) was used to determine the 100% level of membrane permeabilization (38).

TABLE I
NSAID concentrations required for apoptosis, membrane permeabilization, and Ca^{2+} increase

ED_{50} values of NSAIDs for apoptosis (concentrations of NSAIDs required for 50% inhibition of cell viability by apoptosis) were calculated based on results provided in Fig. 1 in the present study and Fig. 2*B* in our previous study (13). ED_{20} values of NSAIDs for calcein release (concentrations of NSAIDs required for 20% release of calcein) were calculated based on results provided in Fig. 2 in the present study and Fig. 4 in our previous study (13). ED_{double} values of NSAIDs for Ca^{2+} increase (concentrations of NSAIDs required for 2-fold increase in the intracellular Ca^{2+} level) were from Fig. 4 in the present study. ND, not determined.

NSAID	ED_{50} of apoptosis	ED_{20} of calcein release	ED_{double} of Ca^{2+} increase
		mM	
Indomethacin	0.6	0.5	ND
Diclofenac	0.8	0.9	0.15
Ibuprofen	1.8	17	0.3
Flurbiprofen	1.2	13	0.6
Ketoprofen	3.2	28	1.2
Mefenamic acid	0.7	3.0	0.5
Flufenamic acid	0.2	1.3	0.08
Celecoxib	0.08	0.02	0.03
Nimesulide	1.6	14	0.55
Etodolac	1.6	15	5.6

NSAID required for 2-fold increase in the intracellular Ca^{2+} level based on results in Fig. 4*A* (ED_{double} value for Ca^{2+} increase in Table I). Compared with ED_{20} values for membrane permeabilization (calcein release), etodolac showed a very high ED_{double} value for Ca^{2+} increase (Table I). Plotting the ED_{double} value for Ca^{2+} increase *versus* ED_{20} values for membrane permeabilization (calcein release) of NSAIDs other than etodolac and indomethacin yielded an r^2 value of 0.738 (Fig. 3*B*), which suggests that increase in the intracellular Ca^{2+} level by most of NSAIDs is mediated through their ability to permeabilize membranes. The membrane permeabilizing activity of etodolac may cause apoptosis independently of the Ca^{2+} increase; however, the mechanism is unknown at present. As well as showing the greatest potency for induction of apoptosis and membrane permeabilization (Figs. 1 and 2) (13), celecoxib increased intracellular Ca^{2+} levels more potently than the other NSAIDs (Fig. 4*A*). We therefore selected celecoxib for use in subsequent experiments.

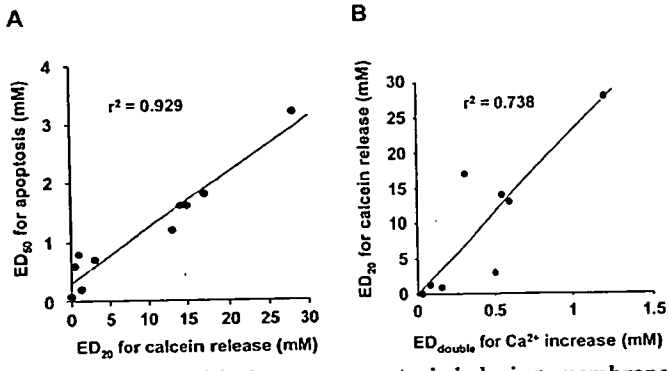

FIG. 3. **Relationship between apoptosis-inducing, membrane permeabilization, and Ca^{2+}-increasing activities of NSAIDs.** ED_{20} values for membrane permeabilization (calcein release), ED_{50} values for apoptosis and ED_{double} values for Ca^{2+} increase are from Table I. All 10 NSAIDs and NSAIDs except etodolac and indomethacin are plotted in *A* and *B*, respectively.

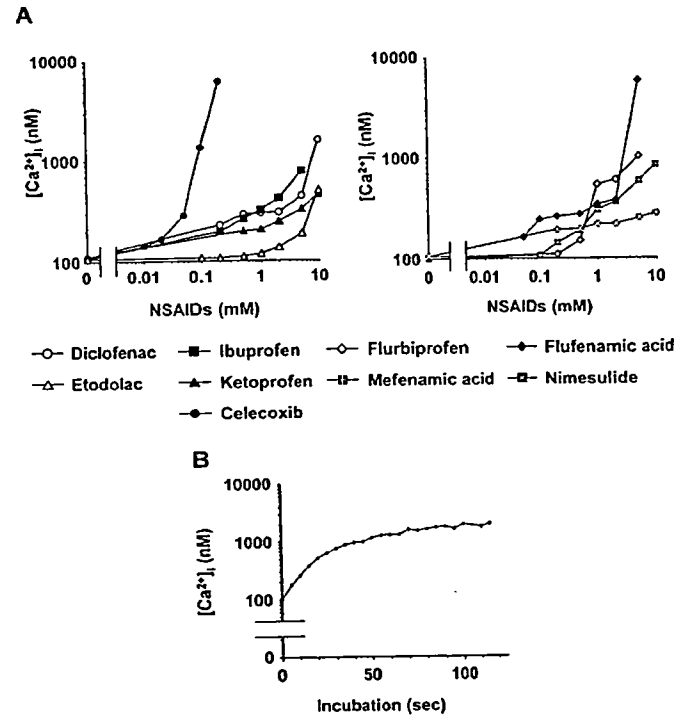

FIG. 4. **Changes in the intracellular Ca^{2+} level induced by NSAIDs.** The intracellular Ca^{2+} level was monitored using a fluo-3/AM assay system. Indicated concentrations of each NSAID were added to fluo-3/AM-loaded cells, and the time course of fluo-3 fluorescence change was monitored. The maximum values for the intracellular Ca^{2+} level ($[Ca^{2+}]_i$) are shown (*A*). The time course of fluo-3 fluorescence change in the presence of 100 μM celecoxib is shown (*B*).

In order to reveal the mechanism by which intracellular Ca^{2+} levels are increased by celecoxib, we monitored intracellular Ca^{2+} levels under Ca^{2+}-free conditions (see "Experimental Procedures"). As shown in Fig. 5*A*, the increase in the intracellular Ca^{2+} level induced by 50–100 μM celecoxib (apoptosis-inducing conditions) was drastically inhibited under Ca^{2+}-free conditions, suggesting that most of the increase is derived from extracellular Ca^{2+} and not from intracellular compartments (such as the ER

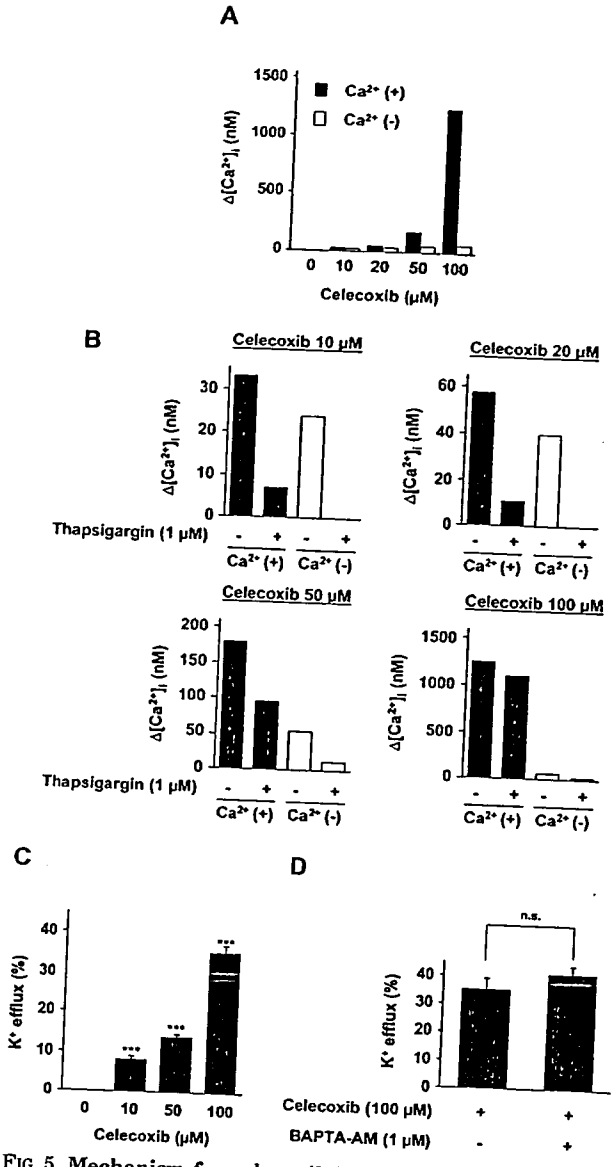

FIG. 5. **Mechanism for celecoxib-induced increases in the intracellular Ca^{2+} level.** Indicated concentrations of celecoxib were added to fluo-3/AM-loaded cells under Ca^{2+}-containing (+) or Ca^{2+}-free (−) conditions (*A* and *B*). Fluo-3/AM-loaded cells were pretreated with 1 μM thapsigargin for 10 min before the celecoxib treatment (*B*). The maximum value for the intracellular Ca^{2+} level ($[Ca^{2+}]_i$) was determined as described in the legend to Fig. 4 (*A* and *B*). Cultured guinea pig gastric mucosal cells were incubated with the indicated concentrations of celecoxib for 30 min (*C* and *D*). Cells were pretreated with BAPTA-AM for 10 min before the celecoxib treatment (*D*). The level of K^+ efflux was measured using a K^+ ion-selective electrode. Melittin (10 μM) was used to determine the 100% level of K^+ efflux (38). Values are mean ± S.E. ($n = 3$). ***, $p < 0.001$; *n.s.*, not significant (*C* and *D*).

and mitochondria). In other words, stimulation of Ca^{2+} influx across the cytoplasmic membrane due to membrane permeabilization by celecoxib seems to be responsible for the increase in the intracellular Ca^{2+} level in the presence of 50–100 μM celecoxib. Since permeabilization of cytoplasmic membranes should stimulate K^+ efflux from cells, we examined the effect of celecoxib on K^+ concentrations in the medium. As shown in Fig. 5*C*, K^+ concentration in the medium was increased, depending on the dose of celecoxib, suggesting that celecoxib stimulated K^+ efflux across the cytoplasmic membranes. These data suggest that celecoxib (50–100 μM) makes the cytoplasmic membranes permeable and stimulates Ca^{2+} influx, resulting in the observed increase in the intracellular Ca^{2+} level.

Since the increase in intracellular Ca^{2+} levels by 10–20 μM celecoxib was not clearly inhibited under Ca^{2+}-free conditions (Fig. 5, *A* and *B*), a mechanism other than stimulation of Ca^{2+} influx across the cytoplasmic membranes seems to be involved. We examined the contribution of the ER Ca^{2+} pool to the celecoxib-induced increase in the intracellular Ca^{2+} levels. Cells were pretreated with thapsigargin, an inhibitor of SERCA, which pumps Ca^{2+} from the cytoplasm to the ER, and then treated with celecoxib under either Ca^{2+}-containing or Ca^{2+}-free conditions (Fig. 5*B*). This pretreatment with thapsigargin depleted the ER Ca^{2+} pool (data not shown). The increase in the intracellular Ca^{2+} level induced by 10–20 μM celecoxib was inhibited more drastically by this thapsigargin pretreatment than by the depletion of extracellular Ca^{2+} (Fig. 5*B*). This contrasts with the results for 50–100 μM celecoxib (Fig. 5*B*). These results suggest that the ER Ca^{2+} pool (and perhaps permeabilization of ER membrane) plays an important role in the increase in the intracellular Ca^{2+} level induced by 10–20 μM celecoxib. In other words, the results indicate that most of the increase in intracellular Ca^{2+} levels that is induced by 10–20 μM celecoxib is derived from the ER and not from extracellular sources. A previous report showed that celecoxib inhibits SERCA (34). Therefore, the inhibitory action of celecoxib on SERCA may also contribute to the increase in the intracellular Ca^{2+} level induced by 10–20 μM celecoxib. In the presence of various concentrations of celecoxib, pretreatment with thapsigargin under Ca^{2+}-free conditions caused almost complete inhibition of the celecoxib-induced increase in intracellular Ca^{2+} levels (Fig. 5*B*). Therefore, both stimulation of Ca^{2+} influx across cytoplasmic membranes and depletion of the ER Ca^{2+} pool are responsible for the celecoxib-dependent increase in intracellular Ca^{2+} levels, which is consistent with previous results (34, 40).

Contribution of the Increase in the Intracellular Ca^{2+} Level to Celecoxib-induced Apoptosis—In order to examine the contribution of the membrane permeabilization and the resulting increase in intracellular Ca^{2+} level to celecoxib-induced apoptosis, at first, we examined the kinetics of celecoxib-induced apoptosis, membrane permeabilization, and increase in intracellular Ca^{2+} level (Figs. 1*B*, 2*B*, and 4*B*). Comparing to induction of apoptosis by celecoxib, the membrane permeabilization (calcein release) and increase in intracellular Ca^{2+} level by celecoxib occurred very rapidly, suggesting that the membrane permeabilization and the resulting increase in intracellular Ca^{2+} level are located upstream of the induction of apoptosis.

We then examined induction of apoptosis under Ca^{2+}-free conditions that is achieved by the addition of BAPTA, Ca^{2+} chelator, to the culture medium. As shown in Fig. 6*A*, the activation of caspase-3-like activity in cells treated with celecoxib for 6 h was partially suppressed by the addition of BAPTA, suggesting that the increase in intracellular Ca^{2+} level by celecoxib is important for celecoxib-induced apoptosis. However, depletion of Ca^{2+} in medium was toxic to cells; treatment of cells with 1 mM BAPTA for 16 h or incubation of cells with Ca^{2+}-free medium decreased the cell viability even in the absence of celecoxib (data not shown). Furthermore, since BAPTA is not permeable for cytoplasmic membranes, BAPTA cannot chelate intracellular Ca^{2+}. In order to address these issues, we used BAPTA-AM, an intracellular Ca^{2+} chelator that is permeable for cytoplasmic membranes. As shown in Fig. 6*B*, BAPTA-AM partially inhibited celecoxib-induced cell death. At the concentrations used, BAPTA-AM did not affect cell viability in the absence of celecoxib (data not shown). Furthermore, treatment of cells with celecoxib caused apoptotic chromatin condensation, which was also partially inhibited by the addition of BAPTA-AM in culture medium (Fig. 6, *D* and *E*).

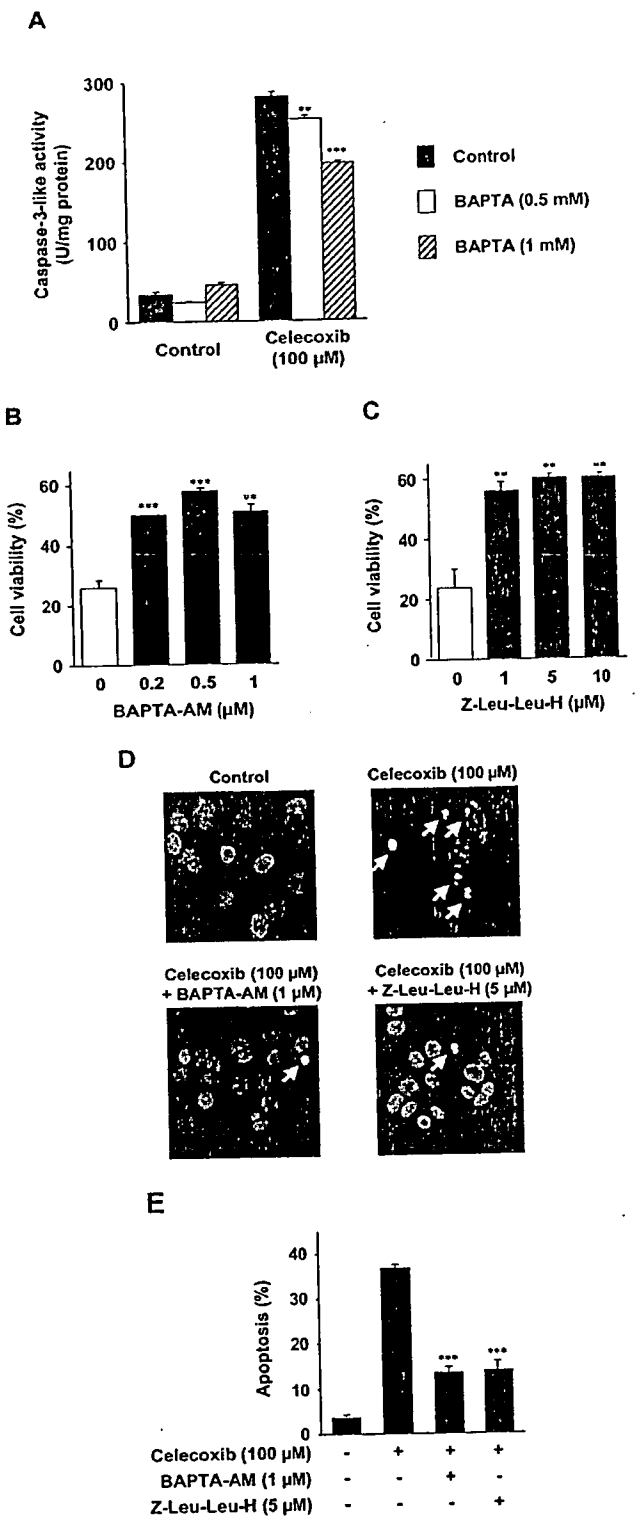

FIG. 6. **Effect of Ca^{2+} chelators or an inhibitor of calpain on celecoxib-induced apoptosis.** Cultured guinea pig gastric mucosal cells were preincubated with indicated concentrations of BAPTA-AM (*B*, *D*, and *E*) or Z-Leu-Leu-H (*C–E*) for 1 h. Cells were further incubated with or without 100 μM celecoxib for 6 h (*A*) or 16 h (*B–E*) under the same conditions as the preincubation step (medium containing BAPTA was used for *A*). Caspase-3-like activity was measured using fluorogenic peptide substrates (acetyl-DEVD-methylcoumarin amide) (*A*). Cell viability was determined by the MTT method (*B* and *C*). Values are mean ± S.E. ($n = 3$). ***, $p < 0.001$; **, $p < 0.01$ (*A–C*). After staining with Ho 342, cells were observed using a fluorescence microscope. The *arrows* show condensed chromatin (*D*). The numbers of apoptotic cells with condensed chromatin were counted from representative photomicrographs and are expressed as a percentage of total cell number ($n = 100$). Values are mean ± S.E. ($n = 3$). ***, $p < 0.001$ (*E*).

Therefore, the increase in intracellular Ca^{2+} levels caused by celecoxib seems to be involved in celecoxib-induced apoptosis. BAPTA-AM did not affect the celecoxib-dependent stimulation of K^+ efflux (Fig. 5*D*), suggesting that the membrane permeabilization by celecoxib is located upstream of increase in intracellular Ca^{2+} level and induction of apoptosis by celecoxib.

We also examined mitochondrial dysfunction in the presence of celecoxib. As shown in Fig. 7*A*, treatment of cells with celecoxib increased the amount of cytochrome *c* in the cytosolic fractions, suggesting that celecoxib stimulated the release of cytochrome *c* from mitochondria. The addition of BAPTA-AM partially suppressed this increase in the amount of cytochrome *c* (Figs. 7, *A* and *B*), suggesting that the celecoxib-dependent release of cytochrome *c* from mitochondria is partly due to the increase in the intracellular Ca^{2+} level.

We also examined mitochondrial dysfunction by monitoring the mitochondrial membrane potential, using DePsipher, a mitochondrial dye. This mitochondrial dye normally exists in solution as a monomer emitting green fluorescence (530 nm) and forms a dimer emitting red fluorescence (590 nm) in a reaction that is driven by the mitochondrial membrane potential. Thus, a decrease in the mitochondrial membrane potential should reduce the red fluorescence. As shown in Fig. 7*E*, the red fluorescence was apparent in control cells (without celecoxib) but was markedly decreased in celecoxib-treated cells. However, when cells were treated with celecoxib in the presence of BAPTA-AM, the red fluorescence was partially recovered (Fig. 7, *E* and *F*), suggesting that the celecoxib-dependent decrease in mitochondrial membrane potential is partly due to the celecoxib-induced increase in the intracellular Ca^{2+} level. These results show that the observed increase in the intracellular Ca^{2+} level is involved in celecoxib-induced mitochondrial dysfunction.

Mechanism for Ca^{2+}-dependent Celecoxib-induced Apoptosis—Then we examined the pathway for celecoxib-induced apoptosis downstream of the increase in the intracellular Ca^{2+} level. First, we examined the contribution of the intracellular Ca^{2+} level to celecoxib-induced CHOP expression, which was shown to play an important role in NSAID-induced apoptosis (19). Treatment of cells with celecoxib increased the amount of CHOP, as was previously reported (19) (Fig. 8, *A* and *B*). However, when cells were treated with celecoxib in the presence of BAPTA-AM, this CHOP induction was partially inhibited, suggesting that CHOP induction by celecoxib is partly due to the celecoxib-induced increase in the intracellular Ca^{2+} level.

We also examined the participation of calpain in celecoxib-induced apoptosis. We found that the activity of calpain was increased in celecoxib-treated cells by use of cell-permeable calpain substrate (Fig. 9). This calpain activation was partially inhibited by pretreatment of cells with BAPTA-AM (Fig. 9), suggesting that this activation is partially due to an increase in the intracellular Ca^{2+} level in the presence of celecoxib. An inhibitor of calpain, Z-Leu-Leu-H, partially suppressed the celecoxib-dependent decrease in cell viability and apoptotic chromatin condensation (Fig. 6, *C–E*). At the concentrations used, Z-Leu-Leu-H did not affect cell viability in the absence of celecoxib (data not shown). These results suggest that calpain is involved in NSAID-induced apoptosis. As shown in Fig. 7, *C–F*, both the celecoxib-stimulated release of cytochrome *c* from mitochondria and the celecoxib-dependent decrease in mitochondrial membrane potential were also partially suppressed by the addition of Z-Leu-Leu-H. From these observations, it is likely that calpain also plays an important role in celecoxib-dependent mitochondrial dysfunction. In other words, activation of calpain by the celecoxib-induced increase in the intracellular Ca^{2+} level seems to damage the mitochondria. On the other hand, in